

HIGH PERFORMANCE MODULAR INSULATING PANEL DEVELOPMENT FOR A REEFER VAN

by

Abdollah Labbani Motlagh

B.Sc., Sharif University of Technology, 2006

Thesis Submitted in Partial Fulfillment of the
Requirements for the Degree of
Master of Applied Science

in the

School of Mechatronics System Engineering
Faculty of Applied Sciences

© Abdollah Labbani 2016

SIMON FRASER UNIVERSITY

Spring 2016

All rights reserved.

However, in accordance with the *Copyright Act of Canada*, this work may be reproduced, without authorization, under the conditions for "Fair Dealing." Therefore, limited reproduction of this work for the purposes of private study, research, criticism, review and news reporting is likely to be in accordance with the law, particularly if cited appropriately.

Approval

Name: Abdollah Labbani Motlagh
Degree: Master of Applied Science
Title: *High Performance Modular Insulating Panel
Development for a Reefer Van*

Examining Committee: **Chair:** Flavio Firmani
Lecturer

Majid Bahrami
Senior Supervisor
Professor

Woo Soo Kim
Supervisor
Assistant Professor

John Jones
Internal Examiner
Associate Professor

Date Defended: April 04 , 2016

Abstract

A new modular insulation panel technology for insulating reefer vans is proposed that can solve some of the problems of traditional methods. New insulating materials with lower thermal conductivity and aging rate are considered to be sandwiched in composite panels to provide better thermal performance in addition to stronger structure. The developed technology can be applied on a variety of commercial vans to improve the quality of insulation while reducing the cost and installation time of the process dramatically. The present method suggests prefabricating of modular insulation panels with accurate size in controlled conditions instead of spraying insulation foam inside the vehicles. In addition, the installation method of modular panels enables the operators to replace the damaged parts of insulation easily with less cost instead of changing the whole insulation in the old method. The MATLAB optimization toolbox is utilized to optimize the thickness of insulation panels based on energy cost and operational conditions. To validate the proposed model, a full-scale prototype is built and installed on a Ford transit connect and tested under road conditions for performance approval.

Keywords: Modular insulating panel; Composite sandwich panel; Reefer van; Thermal performance; Insulation thickness optimization

Acknowledgements

I wish to express my sincere thanks to my senior supervisor, Dr. Majid Bahrami, for his expert, sincere and valuable guidance and encouragement extended to me. Without his guidance and persistent help this dissertation would not have been possible.

I also thank Mr. Marius Haiducu and Dr. Wendell Huttema our research group passionate lab engineers, for their absolute and unconditional help throughout the experimentation of my study.

I take this opportunity to record my sincere thanks to all my friends and colleagues who directly or indirectly, have lent their helping hand in this venture.

Table of Contents

Approval.....	ii
Abstract.....	iii
Acknowledgements	iv
Table of Contents.....	v
List of Tables.....	vii
List of Figures.....	viii
Glossary.....	xi
List of Acronyms.....	xii
Executive Summary	xiii
Chapter 1. Introduction	1
1.1. Importance of Insulation	1
1.2. Background	2
1.3. Research Objective	7
1.4. Outline of the Thesis.....	8
Chapter 2. Literature Review.....	9
2.1. Insulating Material	9
2.1.1. Definition	9
2.1.2. Categories of Insulating Materials.....	10
2.1.3. Properties of Insulating Materials.....	12
2.1.4. Traditional Thermal Insulation Materials	13
2.1.5. Long Term Aging of Closed-Celled Foam Insulation.....	15
2.1.6. Modern Thermal Insulation Materials.....	19
2.1.7. Insulating material Comparison	24
2.2. Sandwich Panels	26
2.2.1. Introduction.....	26
2.2.2. Sandwich Panel Concept.....	26
2.2.3. Design Considerations.....	28
2.2.4. Thermal Insulating Performance of Sandwich Panels.....	30
Chapter 3. Model Development.....	33
3.1. Design Approach	33
3.2. Insulation Thickness Optimization of Foam-Core Sandwich Panel.....	34
3.2.1. Problem Formulation:	36
3.2.2. Methodology	38
3.2.3. Results and Analysis	38
3.3. Web-Core Sandwich Panels.....	44
3.3.1. Problem Formulation	45
3.3.2. Methodology.....	48
3.3.3. Coupling ANSYS with Genetic Algorithm	52
3.3.4. Results and Discussion	54

Chapter 4. Implementation of Modular Insulating Panels	61
4.1. Modular Panels and Attachment Methods	61
4.2. Scanning the Geometry of the Vehicle.....	63
4.3. Scaled Chamber for Experimental Test Setup	68
4.4. Modular Panel Modeling	70
4.5. Full Scale Prototype	76
4.6. Finalizing the Panels and Reefer Installation	80
Chapter 5. Conclusions and Future Works	84
References	86
Appendix A. MATLAB Codes for Optimization.....	90
Appendix B. Air Infiltration Study	94
Model Development.....	94
Experimental Setup	95
Results and Discussion	97
References	99

List of Tables

Table 2-1	Comparison between the common insulating materials.....	24
Table 3-1	Initial parameters and assumption for insulation materials [52].....	35
Table 3-2	Effect of energy cost on the thickness of each insulating layer in mm ($T_{out} = 30^{\circ}\text{C}$).....	39
Table 3-3	Effect of fuel price on operational cost and initial cost of the Ford Transit reefer ($T_{out} = 30^{\circ}\text{C}$).....	41
Table 3-4	Design variables and the associated bounds	46
Table 3-5	Properties of the materials being used in insulation panel design [57,38].....	49
Table 3-6	Genetic Algorithm setting parameters for MATLAB	52
Table 3-7	Results of optimization for different runs of MATLAB	58

List of Figures

Figure 1.1.	World Energy consumption by sector at 2012[5]	1
Figure 1.2.	Commercial reefer vans that are the subject of this project	4
Figure 1.3.	Spraying Polyurethane foam on the interior walls of a reefer van [61]	5
Figure 1.4.	Typical spray foam insulation of reefers and associated issues[11].....	6
Figure 2.1.	Thermal conductivity in porous materials, including conduction through the solid and the gas, and radiation through the pores [15].....	9
Figure 2.2.	Example structure of cellular solids, left: open-cell PU foam; Right: closed-cell PU foam [18]	10
Figure 2.3.	SEM micrograph of glass-fiber mats [19].....	11
Figure 2.4.	The macrostructure of expanded polystyrene [20].....	11
Figure 2.5.	Basic structure of closed-cell foam insulation [12]	15
Figure 2.6.	Aging of closed-cell foam insulation [12]	16
Figure 2.7.	Thermal resistivity versus time for a typical, 25-mm-thick, polyurethane foam specimen [10]	16
Figure 2.8.	Aging of PIR foam core slices due to lateral diffusion [9].....	17
Figure 2.9.	SEM image of commercial ceramic hollow microsphere [26].....	18
Figure 2.10.	Effect of insulated paint on building wall's temperature in thermal image, while one building is painted and the other one not [28].....	18
Figure 2.11.	Honeycomb sandwich panel with fiberglass facing [30].....	19
Figure 2.12.	SEM image of aerogel microstructure [33].....	20
Figure 2.13.	Aerogel above a flame presenting the super-insulating properties [34].....	20
Figure 2.14.	Flexible industrial aerogel blanket with integral vapour barrier for sub-ambient and cryogenic applications [37].....	21
Figure 2.15.	Left: A vacuum insulation panel on top of a traditional foam panel of the same U factor. Right: Components of a VIP [21]	23
Figure 2.16.	Thermal bridge through the laminate around the VIP. Adding a second layer of VIP can reduce this effect [14].....	23
Figure 2.17.	Sandwich panel basic components [46].	27
Figure 2.18.	Web-core sandwich panel at left and corrugated-core sandwich panel at right [48].	28
Figure 2.19.	Left: buckling of the compressed face. Right: Shear failure of the core [46].....	29

Figure 2.20.	Schematic of the foam-core insulating sandwich panel and its sub layers	31
Figure 2.21.	Schematic of the web-core insulating sandwich panel and its sub layers	32
Figure 3.1.	Effect of energy cost on the thickness of insulating layers in mm ($T_{out} = 30^{\circ}\text{C}$).....	40
Figure 3.2.	Effect of outside temperature on the thickness of insulating layers (Fuel price = \$1.3 /lit).	42
Figure 3.3.	Effect of insulation thickness on normalized cost of reefer (with no constraint on the maximum thickness of panel).....	44
Figure 3.4.	Schematic of the reinforcing structure for the insulating panel and associated design variables	46
Figure 3.5.	Temperature distribution contour of two-dimensional analysis for a web-core panel	47
Figure 3.6.	Schematic of applied load and boundary condition to the panel	49
Figure 3.7.	Flow chart of the optimization process	53
Figure 3.8.	Mesh generated in ANSYS [60].....	55
Figure 3.9.	Nodal solution by ANSYS, indicating equivalent stress (Von Mises) of the panel.....	56
Figure 3.10.	Example of the evaluation on the value of the panel height.....	57
Figure 4.1.	Schematic showing the concept of a French cleat [62].....	62
Figure 4.2.	Schematic showing the concept of toggle mechanism [63].....	63
Figure 4.3.	Interior view of the Ford Transit Connect, which is to be insulated for reefer applications.....	64
Figure 4.4.	Schematic of the 3-D scanner working process[64].....	65
Figure 4.5.	Taking the 3-D image of the vehicle interior surface using a HANDYSCAN scanner.....	66
Figure 4.6.	Isometric view of the geometry imported to SolidWorks from the 3-D scanner.....	67
Figure 4.7.	View of the regenerated model in SolidWorks based on the original imported geometry from the 3-D scanner.....	68
Figure 4.8.	Render of a complex panel from the test bed design in SolidWorks	69
Figure 4.9.	Complete model of the printed prototype after assembling.....	70
Figure 4.10.	SolidWorks model of 2-inches-thick modular insulating panels.....	71
Figure 4.11.	Shows toggle mechanism application for holding the side panels with floor panel.....	72
Figure 4.12.	Toggle mechanism for the ceiling panels and the extra edge to keep them on top of the side panels.....	73

Figure 4.13.	Attachment of side panels to the wall by means of small hooks	74
Figure 4.14.	Use of toggle clamps to attach and hold the front panels to the side panels.....	75
Figure 4.15.	Modular insulation panel installation process	76
Figure 4.16.	View of a modeled wooden side panel in SolidWorks.....	78
Figure 4.17.	Wooden side panel for the Ford transit before installation in the vehicle.....	79
Figure 4.18.	Final assembly of wooden panels inside the Ford transit van.....	80
Figure 4.19.	Floor panel after being insulated with closed-cell PU foam.....	81
Figure 4.20.	Rear view of assembled insulating panels covered with FRP facing	82
Figure 4.21.	Side view of the insulated van after installation of the electric refrigeration system.....	83
Figure B.5.1.	Schematic of a scaled down prototype of a Ford transit connect with overall dimensions	95
Figure B.5.2.	Experimental setup of the infiltrated chamber.....	96
Figure B.5.3.	Experimental setup view shows the position of instruments	97
Figure B.5.4.	Temperature distribution inside and outside of the chamber 0.6 s after opening the door.	98
Figure B.5.5.	Average temperature inside the chamber for both the experiment and numerical analysis.....	99

Glossary

\dot{Q}_A	Heat flux (W/m^2)
C_f	Energy cost coefficient ($\$/\text{kJ}$)
E	Young modulus (N/m^2)
R	Thermal resistance ($\text{K}\cdot\text{m}^2/\text{W}$)
T	Temperature (K)
U	Thermal transmittance ($\text{W}/\text{m}^2\cdot\text{K}$)
h	Panel height (m)
k	Thermal conductivity ($\text{W}/\text{m}\cdot\text{K}$)
n	Number of webs
ρ	Insulation cost coefficient ($\$/\text{m}^3$)
t	Thickness (m)
ρ	Density (kg/m^3)
σ_a	Allowable flexural stress (N/m^2)
ν	Poisson ratio

List of Acronyms

APDL	ANSYS Parametric Design Language
BA	Blowing Agent
EPS	Expanded Polystyrene
FRP	Fibre Reinforced Plastic
GA	Genetic Algorithm
ISP	Insulated Sandwich Panel
LTTR	Long Term Thermal Resistance
PIR	Polyisocyanurate
PP	Polypropylene
PU	Polyurethane
PVC	Polyvinyl Chloride
VIP	Vacuum Insulated Panel

Executive Summary

Refrigeration systems consume a significant amount of the power generated in service and reefer vehicles. Reefers distribute most of the chilled and frozen products around the world on a daily basis. Minimizing the heat transferred from the environment to the refrigerated space reduces the cooling load and leads to a tremendous reduction in the operating cost and the environmental impacts such as reductions in particular matter and greenhouse gas emissions. A key to cooling load reduction in all refrigeration systems is devising efficient thermal insulation systems. The focus of this study is to design, develop, and experimentally validate an advanced insulation technology for reefer vans that can address the issues of present insulation systems and improve their thermal and mechanical performance.

Motivation

Laboratory for Alternative Energy Conversion (LAEC) at Simon Fraser University in collaboration with Cool-It Hi-Way Services plan to develop new insulation technology in a collaborative project to not only improve the thermal performance and lifespan of the insulation on the reefer vans, but also to reduce the manufacturing and installation costs of the process. The common insulation method uses a foam core composite construction. Polyurethane (PU) foam with foaming agent is commonly sprayed onto the inside of a truck body. Then a sheet of plywood is installed on the foam. Finally, the assembly is sealed using a fiberglass layer over the plywood faces and the edges and seams of the insulation is caulked with silicone adhesives to protect it from water and gas penetration.

The time-consuming nature of this process makes it expensive and the quality of the final product is highly dependent on the installer's skills. In addition, the thermal conductance of the foam material rises dramatically due to penetration of air and humidity (water vapor) into the cells if the foam core is not completely sealed. The humidity adsorption destroys the thermal performance of the insulation layer, insulation degradation up to 5% a year have been reported in the literature. Furthermore, insulation structure is not repairable, and in the case of van accident or damage, the insulation

system has to be rebuilt from scratch or suffer significantly from thermal losses. The ever-increasing demand for system efficiency mandates comprehensive and systematic research into new insulation materials and installation technologies that can provide better thermal insulation, both at the time of manufacturing and throughout the lifetime of the vehicle.

The focus of this project is to suggest proper insulating methods for reefer utilization of commercial vans that are manufactured for multi-proposed application.

Research objectives

The objectives of this research can be summarized as the following:

- Investigating the available insulating materials, including emerging materials such as aerogel and vacuum insulated panels to find the best option for the application of this study.
- Development of a custom-designed modular insulation panels that can be prefabricated in controlled conditions and are capable of quick installation in the vehicle, an installation time of 1 hour is targeted.
- Optimization of the insulation thickness based on thermal and mechanical performance of panels inside the vehicle.
- Design and construction of full-scaled insulation panel prototype for Ford Transit Connect as the targeted vehicle in this project to validate the structural performance of developed technology.

Methodology

In this thesis, the development of new insulation technology for the application of reefer vans is presented. A comprehensive literature review is performed on the available insulating materials in the market for the application of refrigeration to categorize them based on the required characteristics and compare their benefits and drawbacks. In the next step, the concept of composite sandwich panels is investigated to utilize their benefits such as high strength-to-weight ratio in insulation panel designs. Two different structures of sandwich panels with rigid insulating core and web-core filled by soft insulating material are studied. An optimization algorithm is used to choose the

best insulating material and its optimum thickness for the foam core sandwich panels considering the energy cost and operational conditions. Also, a finite element code in collaboration with genetic algorithm is developed to optimize the structure of a web-core sandwich panel based on the required thermal performance.

Along with conceptual design of modular insulating panels, experimental work on CAD modeling of panels for the targeted vehicle is performed. The interior geometry of the Ford transit van is 3-D scanned and imported into SolidWorks. The proposed model is used to design the modular insulating panels for the vehicle. To validate the practical aspect of the design and structural performance test of the developed insulation panel, a full-scale prototype is built and installed in the Ford transit van and tested under road conditions. An overview of the research project is shown in Fig. 1.

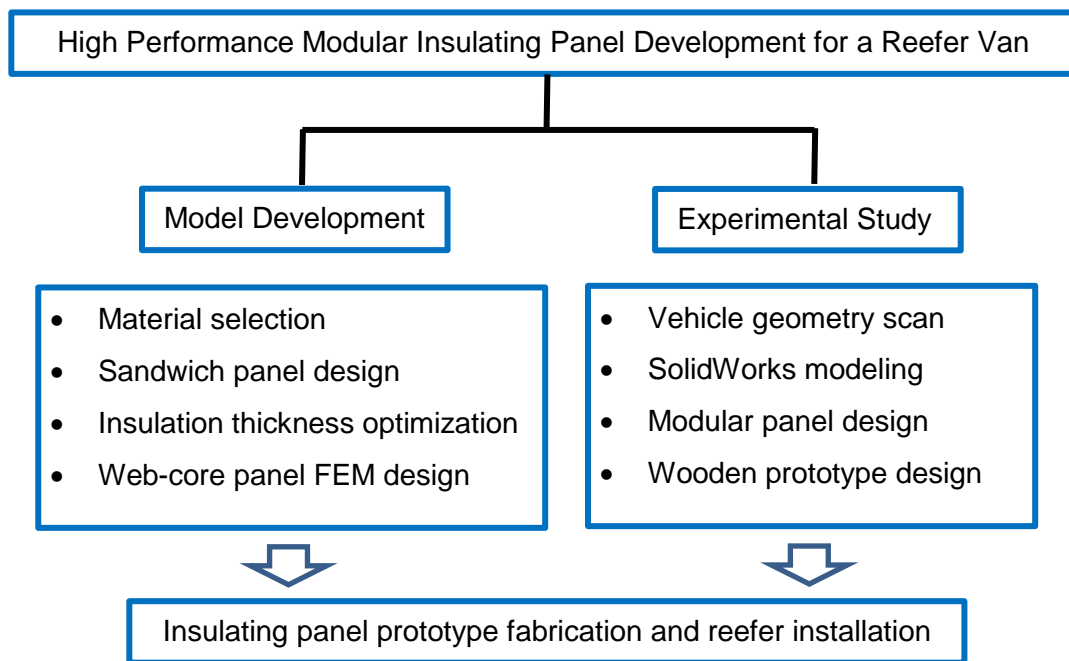


Figure 1: Research road-map

Chapter 1.

Introduction

1.1. Importance of Insulation

Refrigeration systems consume a significant portion of the power generated in reefer trucks, up to 40% [1]. This is a tremendous amount energy usage when one considers the fact that transportation has the biggest portion in world's energy consumption see Figure 1.1. Over a million refrigerated road vehicles and 400,000 refrigerated containers currently distribute a large amount of cooled and frozen products around the world [2] which are responsible for a significant amount of particular matter (PM) and greenhouse gas emissions. In 2000, the US Environmental Protection Agency (EPA) identified diesel PM as a "likely human carcinogen," [3] and followed this with stringent standards call for a 75% reduction in diesel PM by 2010 and an 85% reduction by 2020 from the year 2000 baseline [4]. Any improvement in refrigeration system which reduces the energy and fuel consumption, will impact the greenhouse gas emission and environmental issues in the world.

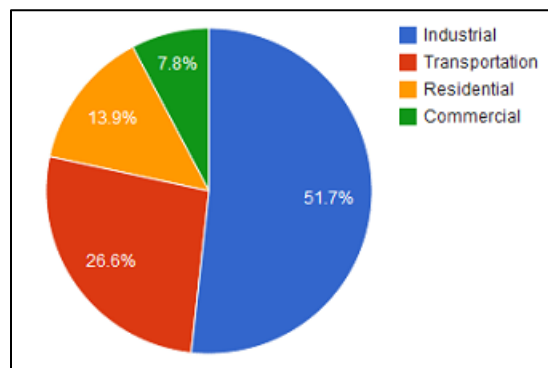


Figure 1.1. World Energy consumption by sector at 2012[5]

Apart from refrigeration industry, HVAC (Heating, Ventilating and Air conditioning) systems can take roughly 40% of total building energy consumption, while 35%-40% of total worldwide energy consumption is considered to be used by buildings [5]. Therefore, any improvement in thermal performance of roof and wall insulation of buildings can significantly decrease the energy consumption in the world.

A key to energy consumption reduction in all HVAC-R systems is devising efficient thermal insulation systems. By minimizing the heat transferred from the environment to the A/C or refrigerated space, the cooling load is minimized leading to a reduction in operating cost and environmental impact.

1.2. Background

According to “Agreement on the International Carriage of Perishable Foodstuffs and on the Special Equipment to be Used for such Carriage” (ATP agreement) [6], an insulated refrigerated truck body for use in the refrigerated food transport industry must have a thermal conductance (U factor) equal to or less than $0.7 \text{ W}/(\text{m}^2 \text{ K})$ and a heavily insulated refrigerated truck body must have a thermal conductance equal to or less than $0.4 \text{ W}/(\text{m}^2 \text{ K})$. These values are measured at the time of manufacturing and do not take into account the effects of thermal insulation decay. The performance decay of some refrigerated truck insulation systems has been shown to be 5% per year [7]. That equates to a 26 to 50% decay in insulation performance over the 10 year lifespan a truck, resulting in up to a 50% increase in the A/C-R loads. Considering the fact that these trucks typically are kept in service for more than 10 years, the problem of insulation decay and the need for a new insulation technology that does not lose its insulation value over time is of critical importance. A reduction in the heat losses into the refrigerated box will reduce the required cooling capacity, and therefore the power consumption of the refrigeration system.

The most commonly used insulation manufacturing method uses a foam core composite (multi-layer) construction. The manufacturing of truck body insulation systems is predominantly performed using one-off production techniques. Polyurethane (PU) foam with cyclopentane foaming agent is sprayed onto the inside of a truck body, then a

sheet of plywood is applied to the face of the foam. Finally, the assembly is sealed using a fiberglass layer over the plywood faces and the edges and seams of the insulation are caulked with silicone adhesives to protect it from water and gas penetration.

Labour and technician time form a large portion of the insulation system's manufacturing costs; due to the large amount of time required to build the insulation system by hand, one truck at a time. The average cost for manufacturing an insulation system is approximately \$8,000 Canadian, not including the base vehicle cost. This process can take up to two weeks and the insulation value of the end product is highly dependent on the skill of the installer. If the insulating foam is of the wrong density or if there are air gaps present behind the plywood panels, the insulation value of the assembly will be poor.

The exact thermal conductance of the foam core varies spatially due to the nature of the installation process, but the average conductance value is $0.022 \text{ W}/(\text{m}\cdot\text{K})$. The high thermal resistance of closed-cell foam is due to low thermal conductivity of the high-molecular-weight blowing agent gas, such as cyclopentane (thermal conductivity of $0.0128 \text{ W}/(\text{m}\cdot\text{K})$ [8]), used during the manufacturing of the foam [1]. The blowing agent gas starts to diffuse out of the cells or dissolve into the polymer matrix during the service life of the insulation and comparatively light-weight air components, such as nitrogen, water vapor and carbon dioxide, start to penetrate into the cells from the environment. Due to the higher thermal conductivity of the invasive air and water vapour over the displaced cyclopentane, the thermal conductivity of the foam rises. Sealing of the foam from the air provides some protection from aging; however, recent research suggests that even with regular sealing, the joints of the structure still age rapidly. Macchi-Tejda et al. [8] found a 9% increase in thermal conductivity in just two years. Mukhopadhyaya et al.[9] observed decay of the thermal resistivity from the initial $50 \text{ m}\cdot\text{K}/\text{W}$ (or $0.020 \text{ W}/(\text{m}\cdot\text{K})$ conductivity) to $40 \text{ m}\cdot\text{K}/\text{W}$ (or $0.025 \text{ W}/(\text{m}\cdot\text{K})$ conductivity) in just 100 days. In the case of prefabricated panels, a variety of impermeable facers, such as aluminum foils, steel sheets, plasterboards, and fiber-reinforced plastics on the surface of the rigid foam may be used to enhance the LTTR (long term thermal resistance) of the boards by protecting the foam from the environment. However, according to research published by the National Research Council Canada (NRC) none of the sealing methods can stop the

aging of foams, and their performance decreases dramatically, by more than 40% after 2 years [10]. Considering the fact that these insulations are typically kept in service for more than 10 years, the problem of insulation decay and the need for new insulation technology that does not lose its insulation value over time are of critical importance.

In the event of a collision, insulation panels are not repairable, and the insulation system has to be rebuilt from scratch or suffer significantly increased thermal losses. The rapid decay of current insulation systems and the ever increasing demand for system efficiency mandates comprehensive and systematic research into new insulation materials and installation technology that can provide better thermal insulation, both at the time of manufacturing and throughout the lifetime of the vehicle.

The focus of this project is to investigate and develop proper insulating methods for commercial vans that are manufactured for multi-proposed application, without insulation on their bodies. Trucks of interest include: Ford Transit, Dodge Sprinter, and Chevy Savana, shown in Figure 1.2.



Figure 1.2. Commercial reefer vans that are the subject of this project

As previously mentioned, the traditional method to insulate these vehicles is to spray polyurethane foam on the interior surface of the refrigerated compartment (Figure 1.3). By installing a layer of plywood on top of the foam and some wooden post at the middle of the foam the mechanical strength of insulation is increased against puncturing

and heavy loads. In the next step, the sealing layer such as aluminum plate, fiber reinforced plastic (FRP) or other food grade plastics is glued or screwed to the wood to make the insulation washable and protect it from water and gas absorption as well as mold growth. Another technique is to build a one-piece fiberglass layer on top of the insulation with glass fibers and thermoset resin. The final step is to use silicon adhesive or some other sealant to caulk the edges and seams. In heavy-duty applications an aluminum checker plate is installed at the end on the floor to make it strong enough for loading skids with a forklift.



Figure 1.3. Spraying Polyurethane foam on the interior walls of a reefer van [61]

The time to insulate a van is 2 to 4 days, depending on the curing time for the material and the capability of the labor force. Labour is the biggest portion of insulation cost, due to time-consuming nature of the work. The quality of the insulation, including the density and the thickness of sprayed foam, is highly dependent on the skill of the workers and can also be affected by ambient temperature and humidity. To make the final surface of the insulation flat, metal ribs on the body of vehicle are either not sprayed or poorly covered, creating thermal bridges through the insulation. Due to complicated geometry of the doors, the insulation is generally poor on doors and large portion of metal is not properly covered (see Figure 1.4). In the case of an accident and damage to the insulation, repair or replacement of the sprayed foam and extra protective layers is

very difficult, so insulation should either be removed completely and rebuilt or the loss in performance accepted until the end of life of the van.

Aging of the insulating material can be a major issue because it causes a reduction in thermal resistance and raises heat load on the refrigeration system. Open-cell foams, which are very common for insulating the reefer vans because of their lower price in comparison to closed-cell, can lose 50% of their thermal resistance in the first year alone due to diffusion of water vapor and other light gases into the foam if they are not completely sealed from the environment [12]. Although closed-cell foams are a better and more expensive insulating material, their thermal conductivity will also rise if placed in humid environment [13]. Condensation of water inside cold rooms provides hard conditions for foam materials and perfect sealing of the paneling is required to avoid decay of the insulation.



Figure 1.4. Typical spray foam insulation of reefers and associated issues[11]

1.3. Research Objective

This thesis presents the process of developing a new insulation system for a reefer vehicle that addresses the issues of present insulation system as mentioned above. To improve the quality of insulation for reefer vans and address the issues with the traditional method, three different areas are considered in this project.

First of all, better insulating materials were studied to choose a better option for this application. Some new materials, such as aerogel and vacuum insulated panels (VIP), with super insulating properties were investigated and compared with typical insulating materials in the market such as polyurethane and glass wool.

Secondly, it is proposed to use modular panels that can be prefabricated in ideal factory conditions with high quality and then assembled on the vehicle at the time of installation. In this way, not only the quality of the insulation panels can be controlled at the time of production and is independent of installer skills, but also labor time and cost will be significantly reduced. In the case of insulation systems using spray foam, insulation will be an inseparable part of the van and it is almost impossible to remove it from the body to facilitate repairs/reconstruction. Thus, modular panels will help users and service providers to repair or replace the damaged panels easily and quickly, with lower cost than building a new insulation system in the traditional way.

Finally, sandwich composite panels attracted a special attention in this project. Insulated sandwich panels (ISP) combine the properties of various materials into a single unit and are commonly used in commercial applications. They are made of different layers to produce a structure with the required properties, such as mechanical strength, thermal resistance and degradation protection. Panels that can be prefabricated would make the installation easier, faster and more reliable.

Although this research investigates a number of different commercial vans to develop a proper insulating system, a Ford Transit Connect was considered as the pilot project for applying all of the proposed ideas and evaluating them in real-world conditions. Therefore, in the experimental part of this project the geometry of a Ford Transit Connect is studied to design suitable insulating panels. After building the scaled-

down prototype to examine some theoretical ideas and heat transfer analysis, a real scale prototype was built based on the design and assembled in the targeted vehicle to show the desired goals of the research. Finally, with the assistance of industrial partner of the project, Cool-It Highway Services, the insulated van was turned into a reefer, with a modern electrical refrigeration system and deployed to verify the capability of the developed insulation system.

1.4. Outline of the Thesis

This work details the structural and thermal design considerations for the modular sandwich insulation panels developed for reefer vans. Because the choice of the core material of the insulating sandwich panel is particularly important, an overview of available insulating materials in the market is presented in Chapter 2. In addition, a brief introduction to composite sandwich panels and their thermal performance is presented in the same chapter. Chapter 3 describes the design approach of the insulating panels for the reefer van and the thickness optimization based on mechanical and thermal considerations. The development process of design and building the real-scale prototype insulating panels for the targeted vehicle is presented in Chapter 4. Validation of the proposed design approach is performed by the installation of insulating panels in the Ford transit reefer, which is described at the end of Chapter 4. Conclusions regarding the use of modular insulating panels and some suggestions for future works are given in Chapter 5.

Chapter 2. Literature Review

2.1. Insulating Material

2.1.1. Definition

Insulation is designed to minimize the heat transfer through a system. It can normally be divided in three parts; solid conduction, gas conduction and radiation through pores. The largest portion of the heat transfer is through solid conduction. Therefore, highly porous materials with a small amount of solid structure make a good insulation material[14]. The radiation importance can increase by lower amounts of solid, as shown in Figure 2.1. Thus, there is an optimal point for a certain material, where the sum of the radiation and solid conduction is at a minimum. In addition, density and conductivity relationship is demonstrated in Figure 2.1.

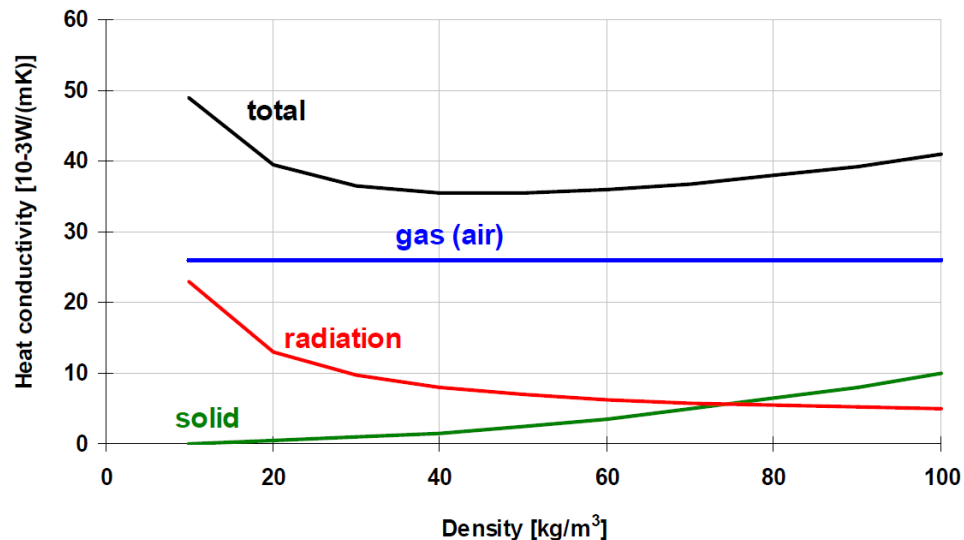


Figure 2.1. Thermal conductivity in porous materials, including conduction through the solid and the gas, and radiation through the pores [15].

Wide variety of insulating materials are available in the market and it is the task of the designer to choose the right product based on his application. Considering the life expectancy of the insulation and requirements of the system, number of products might be satisfying and final decision depends on cost, availability and other considerations [16].

In this section, different common insulating materials for low temperature application are reviewed and their performance properties are discussed.

2.1.2. Categories of Insulating Materials

Insulation materials may be categorized into one of these four major types [16-17]:

1. Cellular Insulations consist of small individual cells that form a cellular structure. A variety of foaming agents can be used to create this structure from base materials such as glass or plastic. Cellular insulations are often classified as open cell (i.e. cells are interconnecting) or closed cell (cells sealed from each other). Generally, materials that contain more than 90% closed cells are considered to be closed cell.

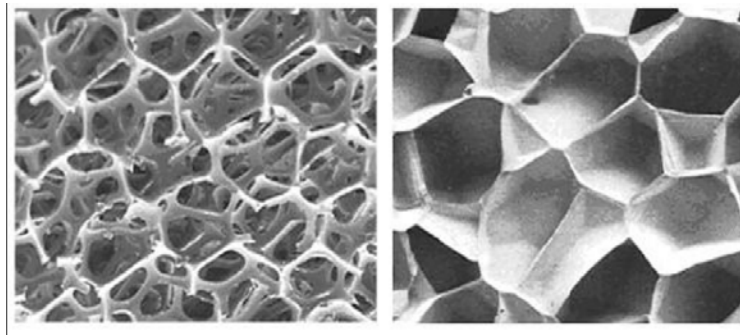


Figure 2.2. Example structure of cellular solids, left: open-cell PU foam; Right: closed-cell PU foam [18]

2. Fibrous Insulations are composed of small diameter organic or inorganic fibers that finely divide the air space and may be held together by a binder. Typical inorganic fibers are glass, rock wool, slag wool, and alumina silica. Fibrous insulations are further classified as either wool, or textile-based insulations that are composed of

woven and non-woven fibers and yarns. Coatings may be applied to these materials for specific properties, e.g. weather and chemical resistance.

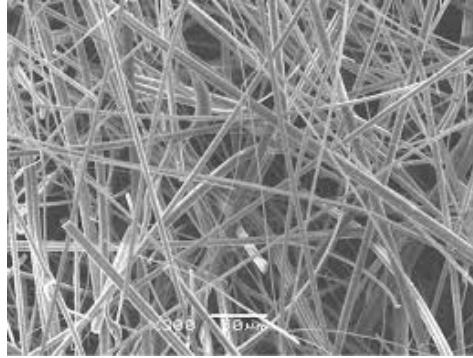


Figure 2.3. SEM micrograph of glass-fiber mats [19]

3. Granular Insulations are composed of small nodules that contain voids or hollow spaces, e.g. calcium silicate and expanded polystyrene insulations. These materials are sometimes classified as open cell materials if gases can be transferred in the material matrix.

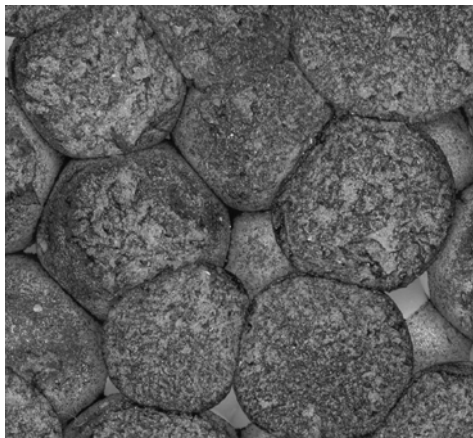


Figure 2.4. The macrostructure of expanded polystyrene [20]

4. Reflective Insulations and Treatments are applied to surfaces to lower the radiant heat transfer to or from the surface. Low emittance facings, such as aluminum foil, are often used in combination with other insulation materials. Thermal insulating coatings or paints are available for use on pipes and buildings 'roofs and are considered

reflective insulation, but there is not much about them in literature to prove their performance.

2.1.3. Properties of Insulating Materials

Understanding the physical properties of available insulating materials is necessary for selecting the proper one regarding the application[16].

Thermal Conductivity is defined as the steady state heat flow through a unit area of a homogeneous material per unit time that is induced by a unit temperature gradient in a direction perpendicular to that unit area. The symbol typically used for thermal conductivity is k or λ and it has units of $W/(m.K)$.

Apparent Thermal Conductivity indicates the presence of additional modes of heat transfer such as radiation or convection. Because thermal conductivity is a function of temperature, in many specifications insulation conductivity is evaluated at a mean temperature of 24°C. Conductivity data may be provided in a range of temperatures to allow consideration closer to the actual working conditions.

Thermal Resistance, or **R-value**, is defined as a unit heat flow rate through a unit area divided by the temperature difference, at steady state, over a specific thickness of material. For a flat insulation, R is calculated as the thickness divided by the thermal conductivity ($R=t/k$). The thermal transmittance, or U-factor, is the inverse of thermal resistance.

Density is the mass per unit volume of a material. For insulation, "bulk" or the "apparent" density of the product is normally important for user. Bulk density is the mass of the product divided by the overall occupied volume. The symbol typically used for density is ρ in units of kg/m^3 .

Specific Heat is the amount of thermal energy required to raise the temperature of a unit mass of a material by one degree that is expressed in units of $kJ/(kg.K)$.

Compressive Resistance is defined as the compressive load per unit of area at a specified deformation. Compressive Strength is start point of complete failure. Compressive strength and resistance are expressed in N/m^2 and are important where the insulation material must support a structural load.

Flexural Resistance is the ability of an insulating block to resist bending and is measured in N/m^2 . Flexural Strength is the flexural resistance at breaking point.

Water Absorption is generally measured by immersing a sample of material under a specified head of water for a specific time period. It is useful to consider the amount of water absorbed due to leaks in barriers or during storage. Water absorption can be measured by variety of immersion methods that differ in immersion time and reported units (% by weight or % by volume).

Water Vapor Sorption is a measure of the amount of water vapor adsorbed by an insulating material under high-humidity conditions. The test includes drying a sample to constant weight and leave it at high humidity condition until the weight stops changing.

2.1.4. Traditional Thermal Insulation Materials

The following is a short description of the most common traditional thermal insulation materials in use today [16,21].

Mineral Wool including glass wool (fibreglass) and rock wool is normally manufactured in mats and boards, and sometime as filling material. The light and flexible products are applicable in insulating the structure of buildings while the harder boards can be used in floors and roofs that mechanical strength is required. The main drawback of these insulating material is absorbing the water vapor and providing proper environment for mold growth.

Glass wool is produced at a temperature around $1400^{\circ}C$, where the heated mass of borosilicate glass is pulled through rotating nozzles and creating fibres. Rock wool is produced from melting stone at about $1500^{\circ}C$, by hurling out the hot liquid from a wheel or disk.

Expanded Polystyrene (EPS) is made by expanding small beads of polystyrene (from crude oil) containing an expansion agent, e.g. pentane C_5H_{12} , at hot water vapor atmosphere. The expanding spheres bond together at their contact areas and create insulation material blocks in a mold or continuous boards on a production line. Typical thermal conductivity of EPS with partly open pore structure is between 35 and 45 $mW/(m \cdot K)$, while varies with temperature, moisture content and mass density. As an example, the thermal conductivity of EPS may increase from 36 to 54 $mW/(m \cdot K)$ with increasing moisture content from 0 to 10 vol% [21].

Graphite Polystyrene is produced by adding graphite to the mixture of EPS that leads to reduction of radiation heat transfer and decrease the thermal conductivity about 20% lower than the conventional material [22].

Polyurethane (PU) is produced by a reaction between isocyanates and polyols (alcohols containing multiple hydroxyl groups). Blowing agent gases such as hydrofluorocarbons (HFC) or cyclopentane, C_5H_{10} that has lower thermal conductivity than air fills the pores of the material during expansion process. PU foam can be formed inside mold or be used as spray foam at the site to fill cavities. Typical thermal conductivity values for PU are between 20 and 30 $mW/(m \cdot K)$, which is lower than glass wool and polystyrene. The thermal conductivity of PU varies with temperature, moisture content and mass density. For instance, the thermal conductivity of PU may increase from 25 to 46 $mW/(m \cdot K)$ with increasing moisture content from 0 to 10 vol%. During a fire PU release hydrogen cyanide (HCN) and isocyanates, which are poisonous [21].

PU foam is supplied in open-cell and closed-cell form. Open-cell foam is soft and weak because the cell walls, or surfaces of the bubbles are broken (Figure 2.2). Thus, the blowing agent gas is not trapped by the forming cells and releases to the atmosphere during expansion and replaces with air. The foam's strength, depends on its closed or open cell structure, enable it to resist liquid water or absorbing water vapour.

Polyisocyanurate (PIR) is an improvement of the polyurethane (PU) by using other substances in the production process. The main improvement is the fire

performance in comparison with PU that produces toxic gasses such as hydrogen cyanide (HCN) and isocyanates in case of fire [21].

Moulded board of PIR is commonly used as insulation in prefabricated panels for roofs, walls, sandwich walls and floors of cold rooms and buildings. PIR also ages similar to PU and its thermal conductivity increases over time from the diffusion of gases. Creating air gaps between the panels inside a structure due to PIR shrinkage can also be an issue [14].

2.1.5. Long Term Aging of Closed-Celled Foam Insulation

While higher thermal resistance (R-value) is in high demand for insulating materials, the overall benefit of them is dependent on their long-term thermal resistance (LTTR) or aging characteristics. The basic structure of closed-cell foam insulation consists of polymer matrix and gas-filled closed cells (Figure 2.5). The blowing agent (BA) fills up the closed-cells and is surrounded by the polymer matrix during the manufacturing process of the foam. The thermal conductivity of the blowing agent that is usually lower than air reduces the gas conduction component of thermal conductivity of the foam [12]. As blowing agent(s) diffuses out of the closed-cells (Figure 2.6) and replaces with air the thermal conductivity of the foam increases over time (called aging).

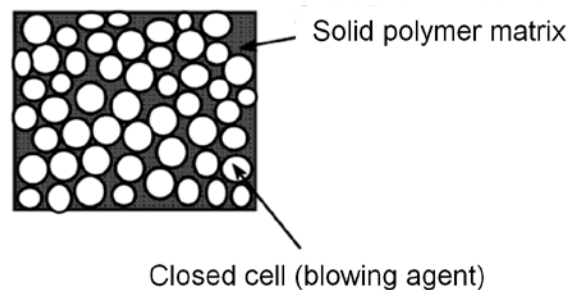


Figure 2.5. Basic structure of closed-cell foam insulation [12]

Parameters such as properties of the foam matrix, geometry and structure of the cells, density, manufacturing process, thickness, and permeability of the surfaces, affect the rate of the diffusion. Before reaching the equilibrium, the aging rate slows down over the time as it is higher after [12].

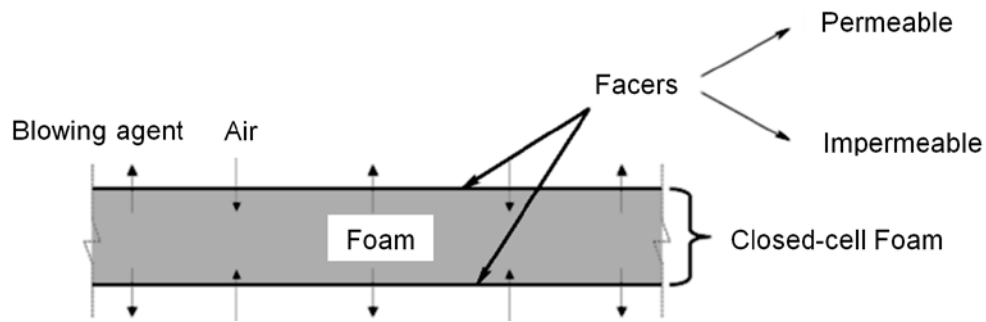


Figure 2.6. Aging of closed-cell foam insulation [12]

Bomberg and Kumaran [24] developed a computer model that explains the aging process of the insulating foam. As shown in Figure 2.7, Curve 1 shows that a 25 mm thick polyurethane specimen that is fully sealed with a coating of epoxy is not affected by aging, as sealing the foam protects it from the entry of air. If air is allowed to enter but the blowing agent redistribution is removed from specific phase, the aging rate is quite high as is shown in curve 2. Adding the effect of blowing agent absorption to previous case results in curve 3. Curve 4 considers the diffusion of blowing agent out of foam matrix in addition to previous affects. This model shows that the biggest change in the thermal conductivity of the foam happens due to penetration of air into the cells [10].

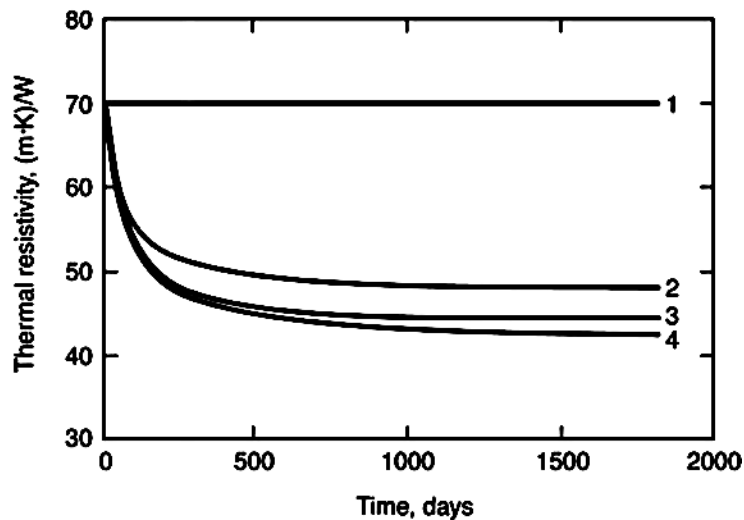


Figure 2.7. Thermal resistivity versus time for a typical, 25-mm-thick, polyurethane foam specimen [10]

Based on a comprehensive research project to determine the LTTR of polyisocyanurate (polyiso) foam insulation board with impermeable facers [9], aging of

PIR foam also does occur due to the lateral diffusion of the blowing agent gas parallel to the facer surface. Foam slices without any facer show a faster aging than PIR foam slices with facer. Also, as shown in Figure 2.8 the aging ratio (the ratio of the thermal resistivity at any specified time to the initial thermal resistivity) of the two-sided 12 mm thick core slice appears to be faster than the one-sided aging of the 6 mm core slice (Figure 2.8).

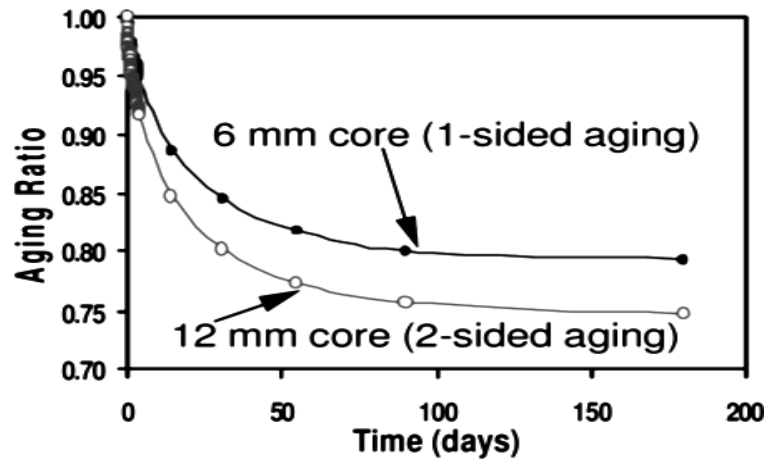


Figure 2.8. Aging of PIR foam core slices due to lateral diffusion [9]

Moreover, research in Foam Supplies, Inc. (FSI) as one of the biggest insulation suppliers in North America has shown that “water vapor diffusion has horrific effects on the thermal conductivity of closed-cell foams” and can increase it to 200% of the initial value in just one week if there is no barrier to protect the foam from water [13].

Insulated Paints consist of ordinary paints that are mixed with ceramic paint additives to insulate and reflect heat. The additives are hollow microspheres that have had all the gas inside of them removed to create vacuum. They help the paint to reflect the heat away from the protected surface and act like barrier that increases the thermal resistance of the paint layer. The tiny ceramic beads look like fine powder in bulk and have inert, chemical resistant properties, which make them an easy material to mix with paint, adhesive or coating to increase the volume of the mixture and decrease heat transfer [25].

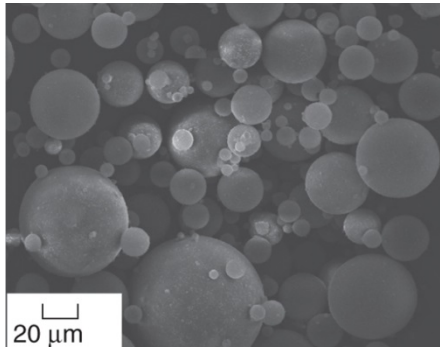


Figure 2.9. SEM image of commercial ceramic hollow microspheres [26]

Insulating additives for paint were originally developed by NASA for the space shuttles but now are commercially used in interior and exterior paint of buildings [27]. By reflecting heat that is capable of passing through walls and the ceiling during summer months, the interior space is kept cooler and in a cold winter heat is reflected back into the living area, resulting in great energy and cost savings. Although the effects of the additives on thermal conductivity and radiation coefficient are not determined comprehensively yet and need more investigation, producers propose an ability to limit as much as 75% heat loss in winter and 93% of heat gain in summer in conventional buildings (Figure 2.10) [28].

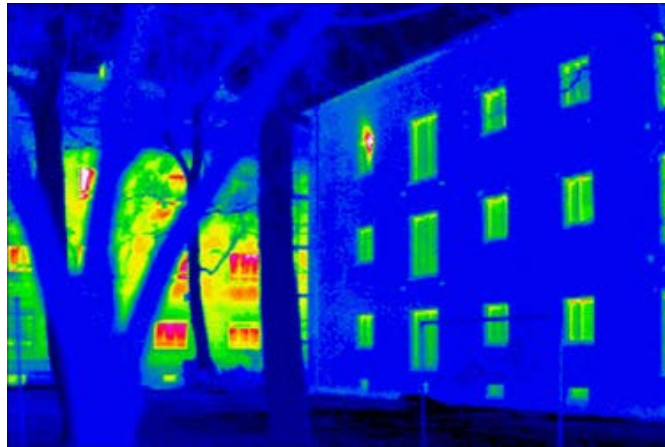


Figure 2.10. Effect of insulated paint on building wall's temperature in thermal image, while one building is painted and the other one not [28]

Honeycomb Structure has the hexagonal form of bee-developed honeycomb, which allows for maximum strength with the least weight. It can be fabricated from different materials, such as paper, plastic, or metals. Plastic honeycomb cores are light, efficient structures that show good insulating properties in addition to mechanical strength and stiffness. Convection can be ignored due to the small size of the cells and conduction through thin plastic walls is very small. Depending on the cell size and wall thickness, thermal conductivity can vary from $0.04 \text{ W}/(\text{m}\cdot\text{K})$ to $0.09 \text{ W}/(\text{m}\cdot\text{K})$ for different type of material, such as polycarbonate, polypropylene, and polyethylene. Honeycomb sandwich panels are constructed from a plastic honeycomb core that is packed between outer fiberglass shells, see Figure 2.11. These composite panels are already in use in truck body manufacturing and are good candidates to be used as floor panels in reefer trucks without supporting beams because of their strong structure and low thermal conductivity [29].



Figure 2.11. Honeycomb sandwich panel with fiberglass facing [30]

2.1.6. Modern Thermal Insulation Materials

In this section some new insulating material with very low thermal conductivity will be introduced. They are gaining a lot of interest recently, especially as their price reduces, due to new and less expensive production methods.

Aerogels are highly porous materials made up of air up to 99.8% and show very low thermal conductivity on the order of $0.004 \text{ W}/(\text{m}\cdot\text{K})$. They are former gel with removed liquid phase and preserved solid structure during the drying [14]. Kistler that

investigated aerogel for the first time [31], heated gel samples to the critical temperature of the liquid while holding the pressure above the vapour pressure. Gel structure will not be damaged by the transition of liquid to gas at temperatures above the critical point. Thus, dry gel was left unbroken and his experiment was successful for different materials [32].

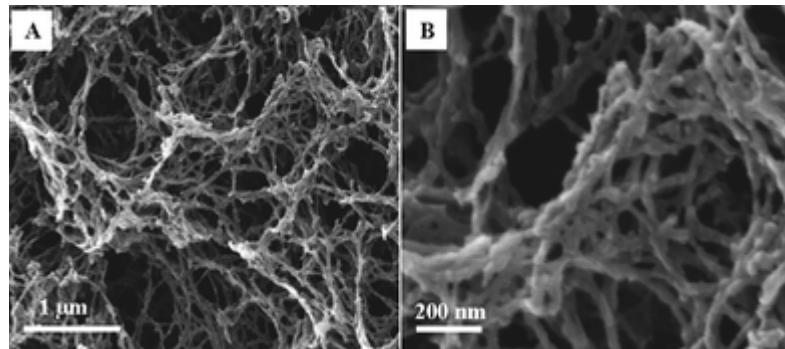


Figure 2.12. SEM image of aerogel microstructure [33]

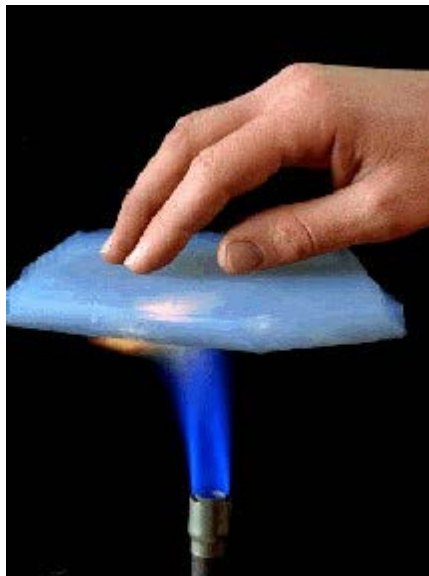


Figure 2.13. Aerogel above a flame presenting the super-insulating properties [34]

Aerogel can be produced as monolithic blocks, as granules with different sizes or as blanket, which is reinforced by some fibrous material. Granular and powder aerogels that showed higher conductivity than monolithic aerogel can be used to fill complex geometry in buildings [14]. Since silica aerogel is mostly transparent, it can be used in

windows as a thermal insulation. Rubin et al [35] tested aerogel windows with transparent aerogel. Radiant conductivity of aerogel can be decreased by applying opacifying agents. Stepanian et al. [36] have patented the aerogel blanket that handle the brittleness problem of aerogel. They claimed reaching conductivities around $10 \text{ mW}/(\text{m}\cdot\text{K})$ at room temperature at their test on reinforced silica aerogel. The proposed composite of a silica aerogel and fibrous reinforcement turns the brittle aerogel into a durable, flexible/solid and hydrophobic material (Figure 2.14).



Figure 2.14. Flexible industrial aerogel blanket with integral vapour barrier for sub-ambient and cryogenic applications [37]

Aerogel blanket shows thermal conductivity of less than $15 \text{ mW}/(\text{mK})$ which is much lower than the traditional insulating foams such as polyurethane [38]. It may be used to insulate the wood-frame or steel-frame building envelopes or insulate the pipelines in cryogenic industries. The current cost of the product is about ten times of the cost of a conventional insulation material to create the same thermal resistance; nevertheless, wherever space and endurance are important considerations, aerogel may be a good option [21].

Although the super insulating properties and flexibility of aerogel blankets provide opportunity for the application of this material in different industries, the properties of aerogel products under various humidity and temperature conditions are still not well-understood and the complete characterization, including thermal resistance decay during temperature and humidity cycling, are under investigation.

Vacuum Insulation Panels (VIP) are another insulator technology that has recently received immense interest. Vacuum insulation panels are a composite construction of two basic layers. The inside core of the composite is an open cell structure, usually fumed silica, but it could also be aerogel or foam, that is surrounded by a sealing membrane (Figure 2.15). The sealing membrane performs three main functions: it seals the core material from the environment, protects the panel from damage and reduces radiation heat transfer [39]. The pressure inside a vacuum filled panel shortly after manufacturing is in the range of 1.33 to 133 Pa. The thermal conductivity of a newly manufactured vacuum insulation panel is on the order of 0.004 W/(m·K). The most common VIP envelope is a metalized multi-layered polymer laminate which is heat sealed to form a continuous envelope. A very important factor influencing the service life of the VIP is the durability of the laminate over time. The insulation ages through reduction in the internal vacuum and infiltration of water vapor. With the use of desiccants and getters, the thermal conductance of a vacuum insulation panel was shown to increase to about 0.009 W/(m·K) over the period of 450 days [39]. The thermal conductance will continue to increase until the internal pressure approaches the ambient pressure, resulting in a maximum thermal conductance of 0.020 W/(m·K) [15]. If the panel is punctured, the thermal conductance instantly jumps up to its maximum value.

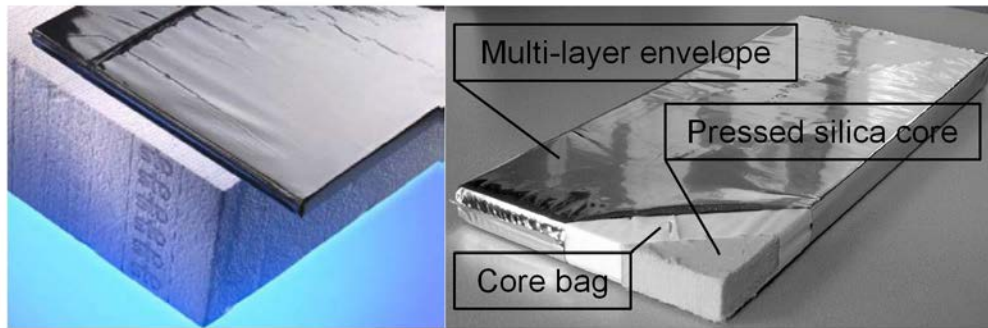


Figure 2.15. Left: A vacuum insulation panel on top of a traditional foam panel of the same U factor. Right: Components of a VIP [21]

The most commonly core material for a VIP is fumed silica, SiO_2 , which is produced from silicon tetrachloride, SiCl_4 . Other materials used in the core are glass wool, polyurethane and polystyrene. The thermal resistance of a material depends on the thermal conductivity of the solid material, convection and gas conductivity in the pores, and radiation between the surfaces of the pores. Fumed silica is significantly heavier than glass wool and polyurethane foam, but has a lower thermal conductivity at higher internal pressure, which increases the service life of the VIP [14].

The laminate film around the VIP creates a thermal bridge because it is composed of metalized multi-layered skin as shown in Figure 2.16. Thermal bridge can be calculated by multiplying the perimeter of panel by the thermal transmittance of the laminate. This value depends on the thermal conductivity values at the center of the panel and laminate, thickness of panel and laminate, and air gaps between the panels [40].

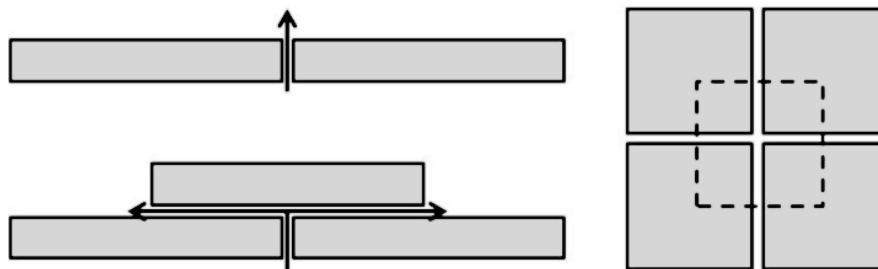


Figure 2.16. Thermal bridge through the laminate around the VIP. Adding a second layer of VIP can reduce this effect [14].

Schwab et al.[41] have performed a complete study on the calculation of laminate thermal bridges using a two-dimensional finite-difference model to calculate the influence of air gaps between the VIP. They showed 360% enhancement in overall heat transfer of an aluminum laminated panel due to laminate thermal bridge.

VIP can easily be punctured during production, storage, or at the time of installation by workers. Visual inspection for loos or wrinkles laminate can detect the damaged panels quickly. VIP found its application first in refrigeration industry and cold shipping boxes as a compact insulating material. However, the expected service life for refrigerators is about 10 years that demands durable insulating materials. It is also an interesting insulation for building application specifically to retrofit the old buildings. Apart from its sensitivity to puncturing, its limited size and thickness due to manufacturing process prevent it from being a conventional insulating material [14].

2.1.7. Insulating material Comparison

In previous section, a brief introduction was made to common insulating materials in the market. To choose the best option for the specific application of this project, a comparison between these materials is necessary to show the pros and cons of each material. A summary of insulating material properties is shown in Table 2-1.

Table 2-1 Comparison between the common insulating materials¹

Material	Density kg/m ³	Thermal Conductivity W/(m·°C)	Thickness for U-factor of 0.7 (mm)	Cost for 1m ² of U-factor 0.7 (CAD)	Disadvantages
Glass wool	10-15	0.04	57	\$2	Weak insulation, flexible
PP honeycomb	60-80	0.04	57	\$29	Expensive, Weak insulation

¹ Prices are from commercial websites: ebay.com, amazon.com, alibaba.com

EPS	10-35	0.035	50	\$6	Weak insulation
Open-cell PU	6.5-15	0.025	36	\$4	Fast aging, low mechanical strength
Closed-cell PU	24-32	0.022	31	\$7	Water absorption, fire hazard
Closed-cell PIR	24-32	0.022	31	\$6	Aging, water absorption
Aerogel blanket	110-180	0.015	21	\$50	Expensive, flexible
VIP	170-190	0.004	6	\$18	Envelope thermal bridge, sensitivity to puncturing

The designer of an insulation system has to consider the thermal and mechanical properties of insulating materials as well as limitations in the production and cost to select the best choice for each part of their system. For example, although honeycomb panels are not very good insulating materials in comparison with other choices, their superior mechanical strength will make them suitable for the floor, since they can tolerate the weight and impacts of goods during loading of reefer vehicles. On the other hand, vacuum insulated panels are very good insulating materials, but they are manufactured only in flat shape and certain rectangular sizes that make it difficult or even impossible to use them for complicated geometries with round or curved features.

Moreover, it can be understood from the table that for the same U-factor, aerogel blanket and VIP are the most expensive insulating materials. Though using these materials make it possible to save some space in cargo compartment of reefer, they will increase the initial cost of insulation by 3 to 8 times that of other insulation types, which may not be acceptable for customers in this industry. Therefore, the designer should keep all of these insulating materials in mind until the design is finalized.

2.2. Sandwich Panels

2.2.1. Introduction

One of the most widely employed materials in the modern world of engineering is sandwich panels. Not only are they suitable in the field of aeronautical construction for which they were initially developed, but also in transportation and marine construction fields [42]. In fact, conventional materials are replacing with sandwich panels in different industrial application due to their high flexural resistance and stiffness [43], high impact strength [44], and low thermal and acoustical conductivity [45]. The design of structures made from sandwich composites is not an easy task, although many research projects have been done in this field. Perhaps, the main reason is that reliable prediction of strength requires in-depth knowledge of the mechanical behaviour of the core and facing materials, as well as damage mechanisms and proper design criteria.

Lightweight sandwich panels are receiving considerable attention in the field of cold storage and refrigerated warehouse facilities in today's food storage industry. Promises of high efficiency, durability and easy fabrication are made by manufactures for the usage of sandwich panels. However, some issues, such as stress creation in panels due to bending as a result of temperature difference between inside and outside of panels, need to be investigated further [46].

2.2.2. Sandwich Panel Concept

Generally, a sandwich panel is composed of two faces and an enclosing core (Figure 2.17). Core material needs to tolerate shear stress and distributed load while facer handle impacts and high mechanical stresses. . A model of an I-beam can be used to describe the behavior of a sandwich panel under bending; the inner and outer faces act as the flange and the core material plays the role of the beam web. Therefore, the presence of a core increases the moment of inertia of the cross section of the beam and the outer faces would be under tension or compression [47]. This model will be very useful at time of design because it explains the mechanical requirement for each part of the sandwich panel.

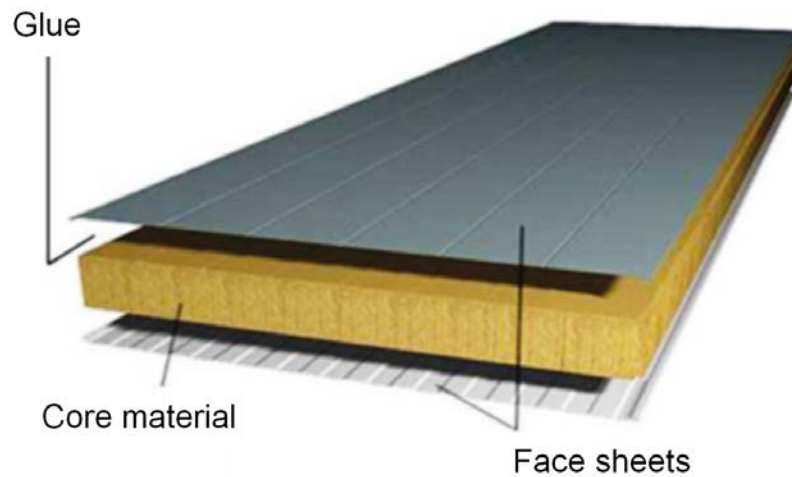


Figure 2.17. Sandwich panel basic components [46].

High strength to weight ratio is the main characteristic of sandwich panels used in the field of refrigeration. Different compositions of materials are used to serve specific functions to provide strength, chemical resistance, thermal insulation, and durability for the structure.

The faces of a lightweight sandwich panel satisfy different requirements. Besides providing beauty and cleanliness, facing materials also provide structural stiffness, which carries stresses caused by a bending moment, and protect the more vulnerable core material from environmental effects and puncturing. A variety of facing materials have been developed for the application of cold room insulating panels, such as stainless steel, galvanized coated steel, aluminum sheet, fiberglass reinforced plastics (FRP), and PVC plastic sheets. The common feature of all these materials is that they are food-safe, washable, and regard the importance of hygiene regulations. The thin faced panels may be classified into flat and lightly corrugated faced panels.

The core of a lightweight sandwich panel is usually glued to the facing and has many functions. It handles the shear or compression stresses based on the applied loading to the structure while facers tolerate the normal stress and impacts. The critical buckling stress and the ultimate compressive strength of the facers can significantly increase by the presence of the core [47]. The core also provides the insulating properties of the system since it usually has the biggest thickness in the panel.

Therefore, selecting the right core material, which is capable of handling the shear stress as well as provide the proper thermal resistance, is one of the key points. Rigid foams such as polyurethane and polyisocyanurate, honeycomb structures made from thermoplastics such as polypropylene, and expandable foams like polystyrene are common insulating materials that are applicable as core material in the field of insulating sandwich panels.

2.2.3. Design Considerations

As explained in the early concepts, the core material is supposed to resist shear deformation due to structural loads. If the sandwich panel is to be an insulating panel, some insulating material cannot play their mechanical role as a core, since they are not strong enough to tolerate the shear stress or compression under loading. For example, aerogel blanket or glass wool bats are not proper materials for the core part of a sandwich panel because they are not rigid solids and will not keep the facings of panels together. Crowley [49] proposed a panel consisting of face sheets and reinforcing webs to address the mentioned problem with soft insulating materials (Figure 2.18). The soft insulating materials fill the space between the structural webs to provide insulating properties for the sandwich panel and no contribution to structural performance. [50]. In this study, the possibility of using a rigid insulating material and soft one have been considered, so the two different designs of the sandwich panel, with or without web-cores, were taken into account.

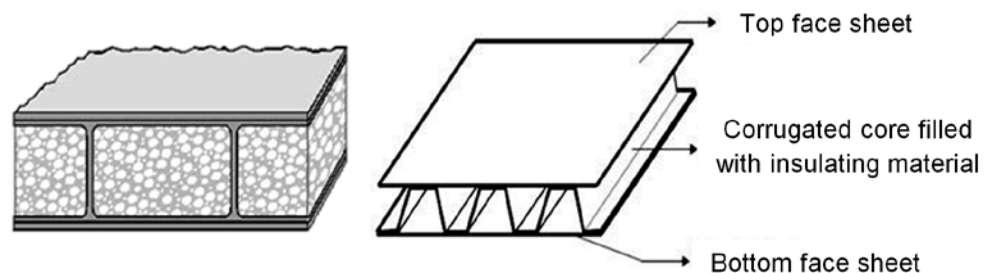


Figure 2.18. Web-core sandwich panel at left and corrugated-core sandwich panel at right [48].

After selecting the proper core design for the sandwich panel, thermal performance needs to be calculated to check if it complies with desire for the project.

Regarding the “Agreement on the International Carriage of Perishable Foodstuffs and on the Special Equipment to be Used for such Carriage” (ATP agreement) [6], an insulated refrigerated truck body for use in the refrigerated food transport industry must have a thermal conductance (U factor) equal to or less than $0.7 \text{ W}/(\text{m}^2\text{K})$. To achieve this goal, the thermal resistance of all parts of the sandwich panel, including faces and webs, has to be calculated. In the next section, the isothermal planes method to calculate the overall thermal conductance of sandwich panel using the analogy of thermal resistors in parallel and series will be discussed.

In addition to the core design of a sandwich panel, the mechanical strength of the panels has to be calculated to ensure they do not fail under the possible loadings. The failure of a sandwich structure can occur through several damage mechanisms such as skin compressive/tensile failure, core shear failure (Figure 2.19), delamination or skin–core de-bonding, core indentation failure, or buckling of the webs [50].



Figure 2.19. Left: buckling of the compressed face. Right: Shear failure of the core [46]

Considering all these failure modes, a structural calculation of the sandwich panels to satisfy the relevant design criteria is beyond this project. However, taking into account the application of panels in this project, it makes the structural calculation much easier. Since these panels are supposed to be installed inside a vehicle, the metal body

of the van would support them mechanically. If the panels attached properly to the rigid walls and roof of the vehicle most of the bending and compression load will be transferred directly to the outer structure and panels can stay safe from mechanical failure damage. Nevertheless, there is another important concern about the failure of the floor panel under the weight of goods that are loaded into the reefer, which has to be calculated based on the maximum vertical load that is allowed to be inserted.

2.2.4. Thermal Insulating Performance of Sandwich Panels

The concept of the isothermal planes method for one-dimensional heat conduction has been discussed completely in [51]. Here is a brief summary that is used in the calculation of the overall heat transfer in sandwich panels.

Based on Fourier's law for conduction, heat transfer in one-dimensional form is

$$\dot{Q}_A = \frac{T_{out} - T_{in}}{R} \quad (1)$$

$$R = \frac{t}{k} \quad (2)$$

where \dot{Q}_A is the rate of heat transfer per unit surface area from the outside into the refrigerated compartment (W/m^2) and T_{out} and T_{in} are the temperature of outside and inside the storage area respectively. R is the thermal resistance to heat transfer through the insulating panel, which depends on t (thickness) and k (thermal conductivity of material $W/(m \cdot K)$). If there is more than one path for heat to transfer through, the amount of R (total thermal resistance) can be calculated based on the analogy for electrical resistors in series and parallel. For example, if there is a compound plate that consists of n layers whose thicknesses are t_1, t_2, \dots, t_n , and whose thermal conductivities are k_1, k_2, \dots, k_n , respectively, and the conduction heat flow rate is common to each layer, then the total thermal resistance of the plate can be calculated as resistors in series:

$$R_{tot} = R_1 + R_2 + \dots + R_n \quad (3)$$

On the other hand, for the heat conduction through a compound layer that consists of n layers of widths w_1, w_2, \dots, w_n , and same thickness, with the heat flow parallel to the interfaces of layers, the total thermal resistance can be calculated as resistors in parallel:

$$R_{tot} = \left(\frac{1}{R_1} + \frac{1}{R_2} + \dots + \frac{1}{R_n} \right)^{-1} \quad (4)$$

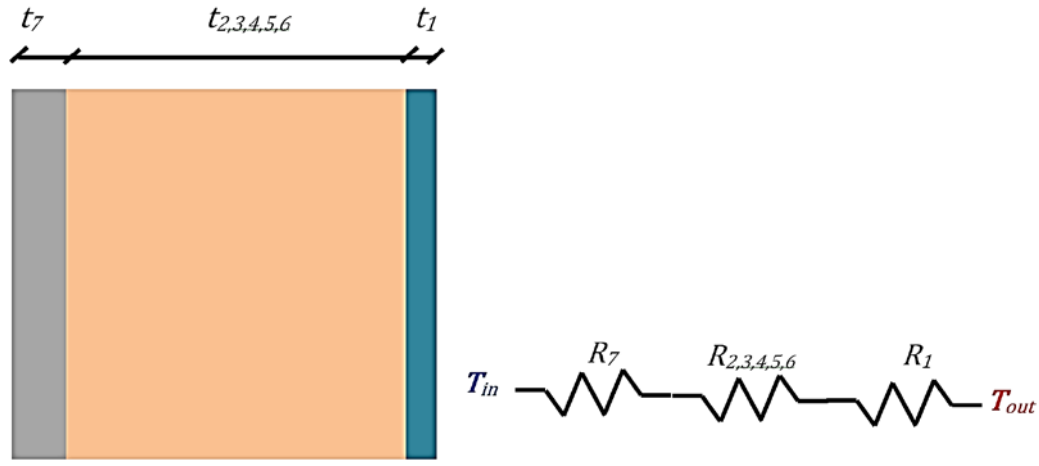


Figure 2.20. Schematic of the foam-core insulating sandwich panel and its sub layers

Based on the above, a foam-core sandwich panel with different sub layers is considered in Figure 2.20. Following the well-known electrical circuit analogy, the thermal performance of the panel assembly is determined by treating the layers as thermal resistances in series.

$$R_{\text{foam-core}} = R_1 + R_2 + R_3 + R_4 + R_5 + R_6 + R_7 \quad (5)$$

For the web-core panels described in this work, the R-value is also determined using the isothermal planes method. In this method, which is illustrated in Figure 2.21, the panel assembly is broken down into a set of layers, defined by (assumed) isothermal interfaces. Following the well-known electrical circuit analogy, the thermal performance of the panel assembly is determined by treating the layers as thermal resistances in series and parallel. The structural layer of the panel is similarly broken down: assuming no lateral heat transfer between the webs and insulating material, these components act as parallel resistances.

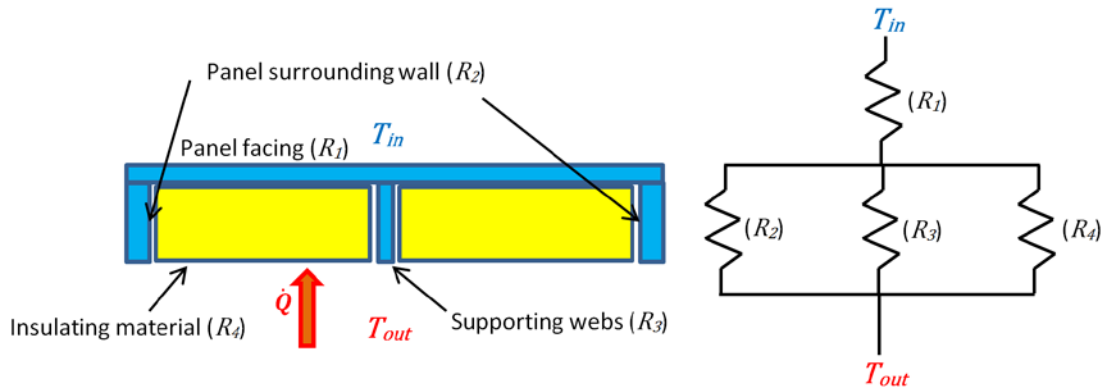


Figure 2.21. Schematic of the web-core insulating sandwich panel and its sub layers

The R-value of the panel assembly is determined from the equivalent thermal resistance of the components:

$$R_{\text{web-core}} = R_1 + \left(\frac{1}{R_2} + \frac{1}{R_3} + \frac{1}{R_4} \right)^{-1} \quad (6)$$

After calculation of total thermal resistance for each case the U factor (the overall thermal conductance) which is the inverse of R with SI units of W/m^2K will be determined. This will be the thermal performance design consideration for the sandwich panel:

$$U = \frac{1}{R_{\text{tot}}} \quad (7)$$

Chapter 3. Model Development

3.1. Design Approach

The analysis and design of sandwich insulating panel requires the simultaneous consideration of thermal and structural performance. As discussed in Chapter 2, there are a few candidates for the insulating material to be used in the sandwich panel structure. In addition, for soft insulating materials that cannot handle the mechanical compression or shear stresses in the panel, a web-core design has to be deployed in order to have rigid structure. Therefore, in the first step a decision about the type of material has to be made, so that it complies with the desired thermal performance needed in this project and then the structure of the panels will be designed.

It is obvious that the selection of insulating material is not only a function of required thermal performance, but will also affect the cost of the product. The financial cost of insulation includes the initial investment in the insulating material as well as exploitation costs, such as the energy cost for the refrigeration system. To keep the balance between these two categories, an optimization process is required to determine the proper insulating material with correct thickness, which will not only comply with the minimum thermal performance of the system, but also minimizes the overall cost of reefer vehicle.

For web-core sandwich panels, since the material of the webs is not a perfect insulation they act like thermal bridges through the core of the panel and the thickness of them is best kept very small to reduce their thermal effects. On the other hand, the thickness and depth of these webs has a key role in the mechanical strength of the panel and larger thickness results in stronger panels. Therefore, there is a challenge in determining the thickness and depth of the webs to design an optimum panel with the right thermal performance and enough rigidity.

3.2. Insulation Thickness Optimization of Foam-Core Sandwich Panel

It is expected the reefer truck will operate while maintaining the cold temperature of the storage area. For typical lifespan of ten years of operation, we aim to minimize the total cost, which is the sum of the initial cost and the operational cost. The initial cost is dependent on the type, thickness and price of the insulation that is used to lower the heat gain of the cabin, while the operational cost is mainly the funds spent on the extra fuel that is fed to the engine to provide power for the cooling system installed in the reefer truck. The fuel that is used to provide power for moving the truck is not being considered in this problem.

In summary, the problem here is designing a proper insulating panel that will keep the balance between the initial cost of insulating material and the operational cost, which is a result of fuel consumption. It is obvious that a low-quality insulation panel will result in higher cooling loads to the refrigerated vehicle, which leads to higher operational costs.

As discussed in previous sections, structure of a foam-core multi-layer insulation panel, which is being used as a thermal shield in a reefer truck, consists of different necessary layers that have different properties such as thermal conductivity, mechanical strength and thicknesses. It should be mentioned that we are not going to consider mechanical strength as a design constraint in this part, and the only parameter that is going to be optimized will be the thickness of each layer, which depends on thermal conductivity and price for the material.

The inner layer of insulating sandwich panels is made of fiber reinforced plastic (FRP) sheet that is rated as a food grade material. The next layer would be the insulating material, which has very high thermal resistance and is the main component that is responsible for minimizing the heat gain in the storage area. This could be any of the following commercialized insulating materials: open-cell polyurethane foam; closed-cell PU; closed-cell (PIR); polypropylene honeycomb structure; or expanded polystyrene (EPS) foam. Finally, the last layer must be made of a material that is capable of sealing the entire panel against moisture and gas diffusion, such as polyvinyl chloride (PVC) or

polypropylene (PP) plastic sheet. Proper installation of this layer is crucial for the system since it can protect the inner material from degradation and can significantly increase the life expectancy of the insulation panel.

The variables in this optimization problem are the thicknesses of these 3 different layers of the insulation panel that potentially can be used to minimize the heat transfer from the environment to the storage area, reducing the total cost of the operation. Initial values for the parameters in the optimization code are given in Table 3-1.

Table 3-1 Initial parameters and assumption for insulation materials² [52]

	FRP	Open-cell PU	Closed-cell PU	Closed- cell PIR	PP honeycomb	EPS	PVC
Thermal conductivity (W/(m·K))	0.3	0.028	0.022	0.022	0.040	0.035	0.15
Life expectancy (years)	10	3	5	5	10	10	10
Cost per 1 m ³ (CAD)	\$5,000	\$90	\$200	\$180	\$500	\$160	\$1,000
Minimum thickness (mm)	2	-	-	-	-	-	1.0

Apart from FRP and PVC that are facing materials for the sandwich panel, it is inferred from the table that PP honeycomb, which is a strong material, is the most expensive insulation material that can be used. PS foam is a traditional insulating

² Prices are from commercial websites: ebay.com, amazon.com, alibaba.com

material that is still commonly used in different refrigeration applications and has the most reasonable price when considering its high mechanical strength in comparison to open-cell PU. Open-cell PU foam is the most commonly used material since it has a quite a low thermal conductivity and low price, but its life expectancy is also low due to fast degradation.

It should be noted that the inside temperature is fixed at the desired level which is 0°C since the product in the reefer should be kept below freezing.

3.2.1. Problem Formulation:

Formulation of a problem is the most important step in optimization and without taking this step properly and carefully, one might face multiple issues in optimizing and finding the optimum solution of function. The concept of problem formulation is introduced in Ref. [53].

By calculating the heat gain of the refrigerated compartment, one can predict the cost of the energy that is consumed to provide the cooling in a refrigeration system. The energy cost depends on different parameters such as the type of refrigerating system, the type and size of the vehicle, road conditions and the cost of fuel per litre in each region. Therefore, for ten years of operation, which is a desired lifetime for a reefer van, the total cost can be introduced as the sum of energy cost and price of insulation, which is the initial cost.

$$\mathbf{Cost} = \mathbf{Energy\ cost} + \mathbf{Insulation\ material\ cost} = C_f \times \dot{Q} \times t_w + \sum_{i=1}^n t_i p_i \times \frac{lt}{d_i} \quad (8)$$

Where C_f is the energy cost, \dot{Q} is the rate of heat load and is calculated based on Equation (1) , t_i is the thickness of each layer of insulation and p_i is the price of insulation, lt is the expected lifetime, which is 10 years , d_i is the degradation time for each type of insulation, and t_w is the working time of the reefer during its life. t_w can be calculated based on the expected lifetime (lt) and working schedule of the reefer. For example, if it is assumed that the reefer only works during summer time (about 100 day a year) and each day 8 hours, t_w would be calculated as:

$$t_w = l_t \times \frac{100 \text{ days}}{1 \text{ year}} \times \frac{8 \text{ hours}}{1 \text{ day}} \times \frac{3600 \text{ sec}}{1 \text{ hour}} \quad (9)$$

Thus, the objective is to minimize the total cost of operation for ten years plus the initial cost. C_f is calculated based on the fuel consumption of the vehicle, dollar-cost of fuel and output power of the engine [54]. If the targeted vehicle in this project (Ford Transit) is considered with 8 lit/100km fuel consumption in the road at the speed of 100km/hour to produce 75 kW (100 horsepower) output power on the wheels and fuel cost of 1.3 \$/lit, the C_f would be calculated as:

$$C_f = \frac{8 \text{ lit}}{100 \text{ km}} \times \frac{100 \text{ km}}{1 \text{ hour}} \times \frac{1 \text{ hour}}{3600 \text{ sec}} \times \frac{1 \text{ sec}}{75 \text{ kj}} \times \frac{1.3 \$}{\text{lit}} = 3.8 \times 10^{-5} \frac{\$}{\text{kJ}} \quad (10)$$

It is obvious that this amount is just a sample to show the estimation and depends on the transportation area, economy condition, and reefer service schedule.

There are some constraints in this problem including the minimum thickness of PVC and FRP layers since layers provide the essential mechanical strength for the insulating panel, and are mentioned in Table 3-1. The total thickness of the insulating panel must be less than 55 millimetres due to limited space available in the refrigerated compartment.

In summary, the optimization problem is:

$$\text{Min } f = C_f \times \dot{Q} \times t_w + \sum_{i=1}^n t_i p_i \times \frac{t}{d_i} \quad (11)$$

Subject to:

$$\begin{aligned}
t(1) + t(2) + t(3) + t(4) + t(5) + t(6) + t(7) - 0.055 &\leq 0 \\
-t(1) + 0.001 &\leq 0 \\
-t(3) + 0.005 &\leq 0 \\
-t(7) + 0.002 &\leq 0 \\
-t(1, 2, 3, 4, 5, 6, 7) &\leq 0
\end{aligned} \tag{12}$$

3.2.2. Methodology

MATLAB [55] is a software package that is frequently used for optimization, since it has a strong toolbox containing very useful functions such as ‘fmincon’ to solve constrained optimization nonlinear problems. This function uses a sequential quadratic programming method to solve a quadratic programming sub problem at each iteration. Fmincon updates an estimate of the Hessian of the Lagrangian at each iteration using the BFGS formula and performs a line search using a merit function [56]. In this study, “fmincon” will be used to find the optimum point for the objective function since the cost function is nonlinear and constrained. The default settings of the “fmincon” function yield reliable results, so the settings have not been changed from default in this study. To exploit the “fmincon” function, it is required to define the objective function and its constraints in the proper way. Therefore, three different MATLAB files were created. The first of these three contains the run file while the other two define the constraints and the objective function. For more details, please refer to the Appendix A of this report.

3.2.3. Results and Analysis

The final cost depends on many variables, such as the outside and inside temperatures, the unit price of each insulating material and the fuel cost. In order to better understand the effect of different parameters we need to change one variable while keeping the others fixed. Since the outside temperature and the energy cost vary in different regions and at different times of the year, it has been decided to perform a parametric study on the effects of these parameters on the insulation thickness. The results are gathered in Table 3-2.

Table 3-2 Effect of energy cost on the thickness of each insulating layer in mm ($T_{out} = 30^{\circ}\text{C}$)

Energy cost (\$/kJ)	FRP	Open-cell PU	Closed-cell PIR	Closed-cell PU	PP honeycomb	EPS	PVC
5.0E-06	2	0		0	0	30	1
1.0E-05	2	0		0	0	43	1
2.0E-05	2	0	0	0	0	52	1
4.0E-05	2	0	12	0	0	40	1
6.0E-05	2	0	35	0	0	17	1
8.0E-05	2	0	52	0	0	0	1

It is obvious from Table 3-2 that the insulating material and its thickness are greatly dependent on energy cost. Not only does the higher energy cost affect the operating expense but it forces the manufacturer to use more expensive and high quality insulation as well. Also, the optimization code always tries to keep the thickness of PVC, and FRP layers at minimum due to their very high cost in comparison with insulating materials. To have a better understanding of this phenomena and see how the optimizer switches from low-quality insulation to high-quality, the results are shown on Figure 3.1. It is shown that as the fuel cost goes higher, the thickness of better insulation material (in this case PIR) increases and low quality insulation gets thinner.

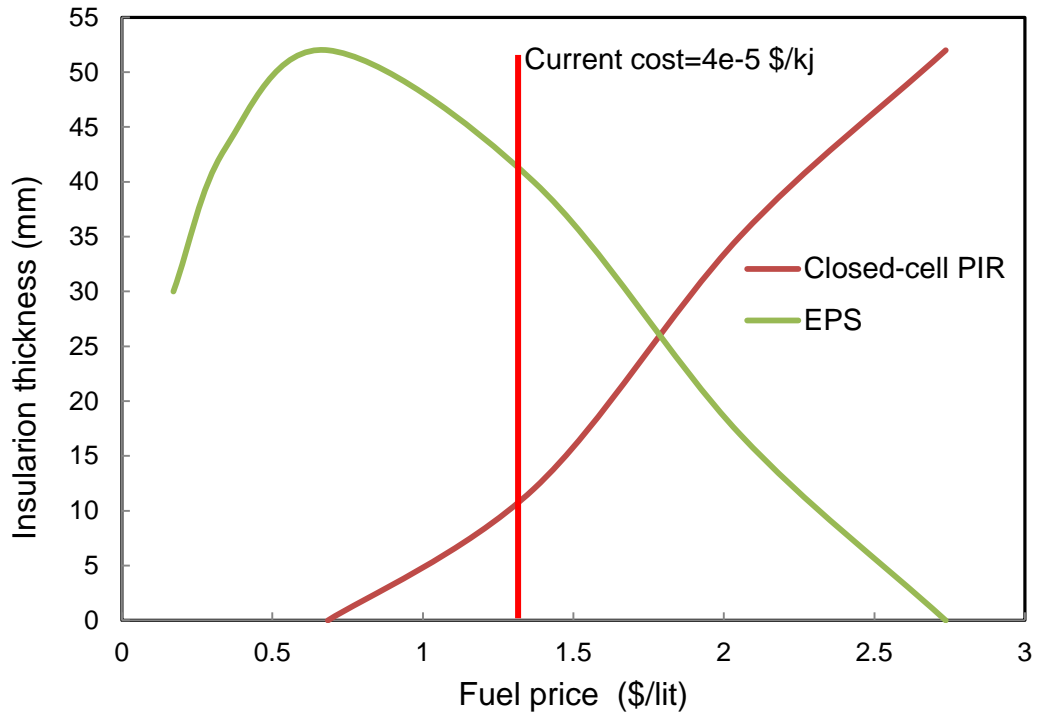


Figure 3.1. Effect of energy cost on the thickness of insulating layers in mm ($T_{out} = 30^{\circ}\text{C}$)

Moreover, the overall thickness of insulating panel is calculated to be 55 mm, which is the maximum, and it shows that no matter what type of material has been used, it is more economical to invest more on insulation since it will reduce the fuel consumption. Only if the energy cost is very cheap, as in the left side of the graph, does it makes sense to use a smaller thickness of insulation.

It was discussed before that better insulation requires high initial cost or bigger investment while cheap insulation will result in high fuel consumption or bigger operational cost. To see this phenomenon, the targeted vehicle of this project (Ford Transit Connect) with average reefer surface area of 20 m^2 is considered. Based on the optimization results for different fuel price, the operational and initial cost of the reefer are calculated as in Table 3-3.

Table 3-3 Effect of fuel price on operational cost and initial cost of the Ford Transit reefer ($T_{out} = 30^{\circ}\text{C}$)

Fuel price \$/lit	Operational cost	Initial Cost	Total cost	Operational cost portion %
0.17	\$100	\$320	\$420	23.81
0.34	\$140	\$360	\$500	28.00
0.68	\$240	\$380	\$620	38.71
1.37	\$400	\$440	\$840	47.62
2.05	\$500	\$520	\$1020	49.02
2.74	\$580	\$600	\$1180	49.15

At the first rows of the table, the fuel price is quite low and consequently the operational cost has the smaller portion of the total cost. As the fuel price raises toward the bottom of the table, initial cost and operational cost both increase. Operational cost is a direct function of fuel price while the initial cost will be bigger since the optimizer tries to compensate the effect of energy cost by adding more thermal insulation to reduce the load on the system. However, the rate of operational cost expansion is faster than initial cost and at the bottom of the table, it reaches the 50% of total cost of the reefer.

It should be noted that dollar amounts shown in Table 3-3 are the net costs based on some assumptions and estimations. These values would be different from the real amounts and should not be considered as final cost of the project. For example, to manufacture the insulating panels in specific size and shape of the vehicles there is always some scraps or leftover which raises the cost of initial material. Also, manufacturing process and labour cost can be more expensive than the required material for the panels. On the other hand, the energy cost of the reefer is a portion of fuel cost for the vehicle and in this study is calculated only for the warm days of the year (100 days assumption).

In Figure 3.2, the energy cost (fuel price) was kept constant to see the effect of outside temperature change on the insulation material. In fact, because the inside temperature is fixed at 0°C , this figure shows the effect of temperature difference between inside and outside. It is inferred from the figure that by reducing the outside

temperature, the thickness and quality of insulation can decrease, which makes sense. Thus, by running in colder climates the cost would be decreased. The other interesting result is that the optimization code always chooses between two materials, EPS and Closed-cell PIR. The first one is the cheapest insulating material and the second is the best quality insulating material with a lower price. Although the unit price of open-cell PU is less than EPS, the optimizing code prefer to use the EPS instead of open-cell PU. The reason is that the lifespan of open-cell PU is less than operational life of the reefer vehicle (10 years) and the insulating material needs to be replaced after that or the heat transfer from outside will be increased gradually, which raises the energy consumption as well. Since the algorithm just considers the total cost of project it cannot see the advantages of the other material, such as the better mechanical strength of PP-honeycomb panel, and the designer has to consider these issues.

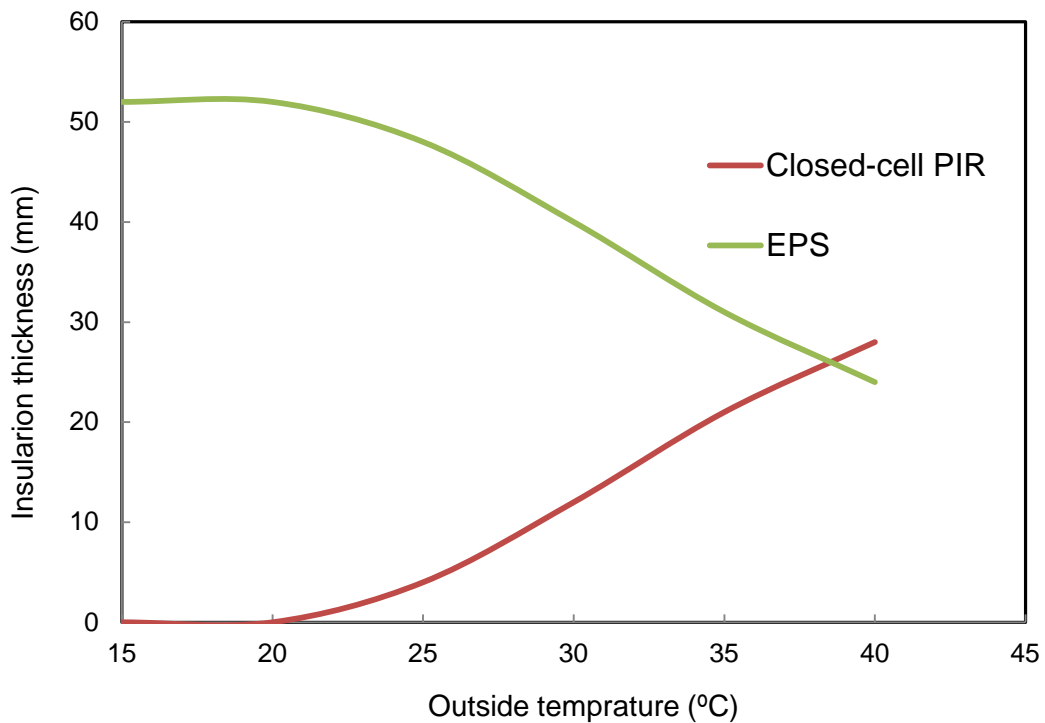


Figure 3.2. Effect of outside temperature on the thickness of insulating layers (Fuel price =\$1.3 /lit).

It will be better for the environment to invest in the insulation instead of paying for the consumption of fuel. However, what would be the optimum thickness of insulation for this project? To answer this question, the conditions in a particular area have to be considered. For example, if the average outside temperature is 25°C and energy cost is 4e-5 \$/kJ (current energy cost based on the average cost of gas around 1.3 \$/lit), the result would be 48mm of EPS plus 4mm of closed-cell PIR. The thermal resistance of the panel in this case is 1.56 that is equivalent to the U-value of 0.64 W/(m²K) which is lower than the acceptable value mentioned from APC agreement (0.7 W/(m²K)).

In addition, shifting the constraint on the maximum thickness of the panel, which is 55mm, has direct effect on the results. With 100mm constraint on the maximum thickness and same condition for temperature and fuel cost, the result is 79mm of EPS that is equivalent to U-value of 0.44 W/(m²K). In fact, if there is no maximum limit for the thickness of the panel then 79mm of EPS will be the best insulation that minimizes the overall cost of reefer. This phenomena can be seen in Figure 3.3 that shows the effect of insulation thickness on normalized values of insulation and operational cost of reefer where there is no limit on the maximum thickness of panel. As the insulation thickness changes from the optimum value (79mm of EPS), the total cost increases.

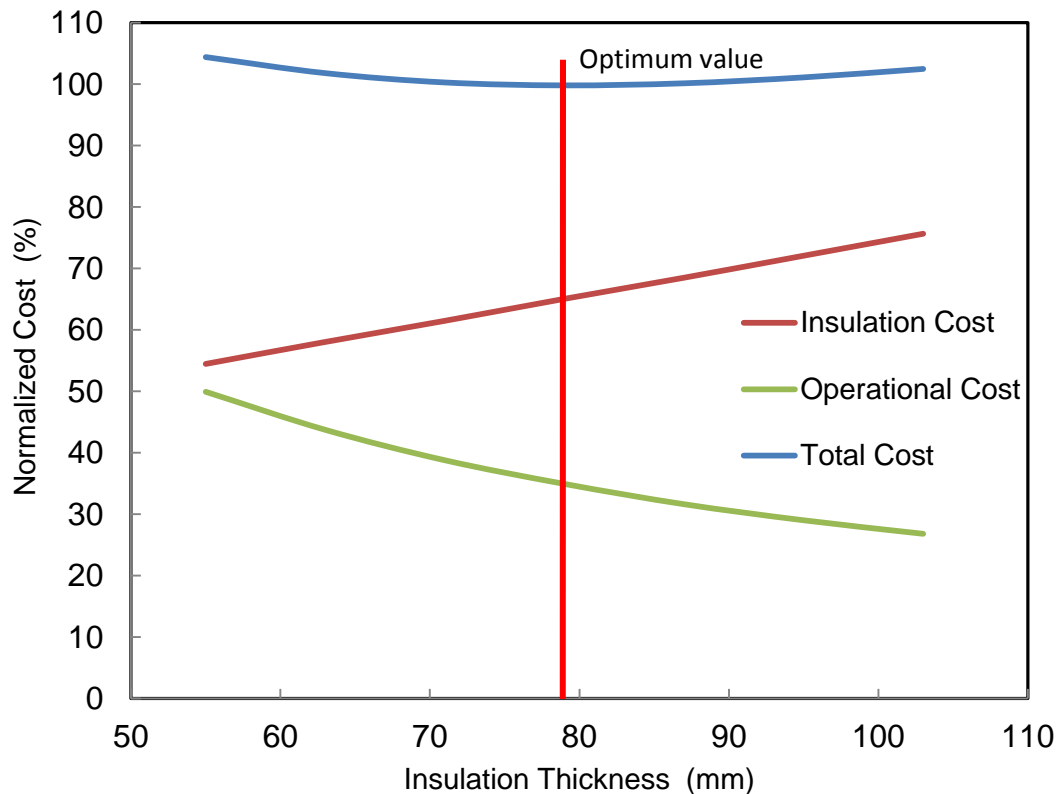


Figure 3.3. Effect of insulation thickness on normalized cost of reefer (with no constraint on the maximum thickness of panel)

On the other hand, tighter constraint on the maximum thickness of the panel would force the optimizer to use more efficient insulating material in the provided space. For example, defining maximum thickness of 30mm urges the optimizer to recommend closed-cell PIR as the proper insulation.

3.3. Web-Core Sandwich Panels

The decay of currently utilized foam insulation systems and the ever increasing demand for system efficiency mandates comprehensive and systematic research into new insulation materials. As was shown in the previous section regarding increasing energy costs, high quality insulating material has to be employed to reduce the operational cost of refrigerated vehicles. It was also discussed that super insulating materials such as aerogel and vacuum insulation panels cannot tolerate the mechanical

stress in ordinary sandwich panels and web-core sandwich panels were invented to solve this problem. The webs, which are working like reinforcing webs among the insulating material, increase the rigidity of the panel. Although the number of webs and their thickness play key roles in panel strength, they would also change the thermal resistance of the panel in the opposite way since they act like thermal bridges between the two sides of the panel. Therefore, these parameters have to be designed in such a way to provide the required efficiency for the insulation panel, both thermally and structurally.

3.3.1. Problem Formulation

In this section, a proper geometry for the reinforcing structure will be chosen and optimized in order to have the smallest thickness of the panel while maintaining a satisfactory mechanical strength and thermal performance. The main reason to reduce the height (overall thickness) of the panel is decreasing the cost of insulating material. As it mentioned before, aerogel blanket is one of the most expensive insulating materials in the market and its application will have significant impact on the initial cost of the reefer. Obviously, smaller height of the panel would save some useful space in cargo area of the reefer and might lower the weight of the panel and its manufacturing cost as well.

In Figure 3.4, the insulation panel is shown to consist of a plastic tray with reinforcing webs in the back. The insulating material fills in the space between the webs. The length and width of the insulating panel unit are fixed (1m x 0.5m) while the thicknesses shown in Figure 3.4 and the number of webs in each direction (n_1 in the length and n_2 in the width) are the design variables that should be optimized to gain the minimum thickness of the panel while maintaining the thermal resistance above the design value and the maximum stress in the allowable range (Table 3-4).

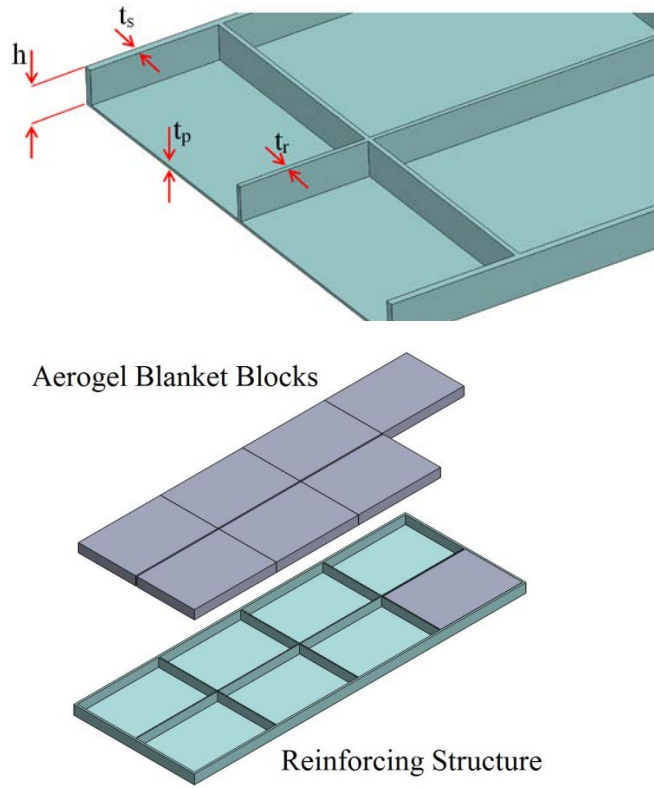


Figure 3.4. Schematic of the reinforcing structure for the insulating panel and associated design variables

Table 3-4 Design variables and the associated bounds

Variables	h (mm)	t_p (mm)	t_s (mm)	t_r (mm)	n_1	n_2
Lower bound	20	1.5	1.5	1.5	1	1
Higher bound	55	6	6	6	5	3

Since our application requires the reefer truck to be heavily insulated to minimize the costs associated with cooling the truck, the U factor value of $0.5 \text{ W}/(\text{m}^2\text{K})$ has been chosen to be the constraint on thermal performance of the insulation panel, a lower value than is demanded in ATP agreement. In addition, this value can provide the opportunity to compare the results of this section with previous one to see which core

structure and material would work better for this project. To calculate the U factor for the reinforced insulation panel, one-dimensional heat conduction was considered as is shown in Figure 2.21. The total thermal resistance of the panel can be calculated based on equation (6) and then the U factor is the inverse of R. Because the goal is to have an insulation panel with U factor less than 0.5 W/(m²K) for any combination of design variables including number of webs and the thickness of panel in different areas, this constraint has to be considered during analysis:

$$U = \frac{1}{R_{tot}} < 0.5 \frac{W}{m^2K} \quad (13)$$

In reality, the heat transfer through the web-core panel is two-dimensional which is not easy to calculate theoretically. To justify the one dimensional calculation for the case of this study, a FEM analysis was performed on a two-dimensional model of a PVC panel with aerogel insulation that is exposed to 25 °C of temperature difference between the both sides. Result for temperature distribution inside the panel is shown in Figure 3.5.

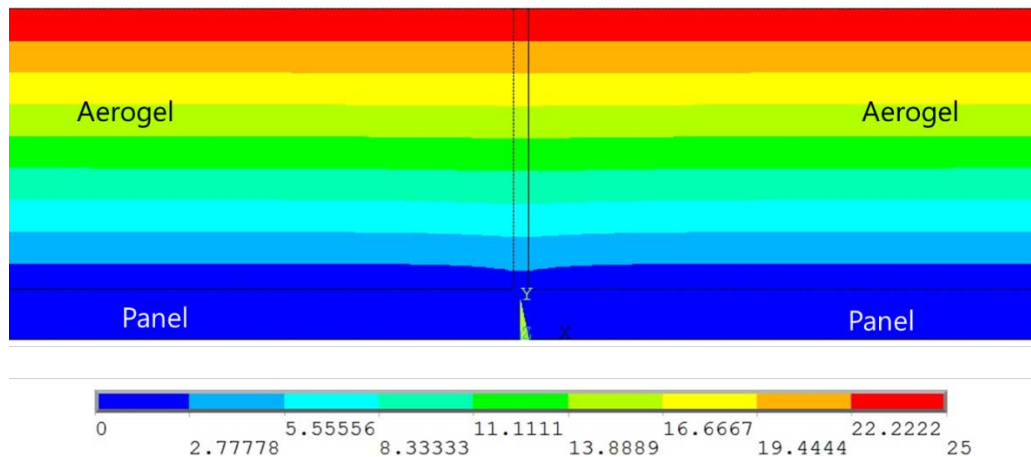


Figure 3.5. Temperature distribution contour of two-dimensional analysis for a web-core panel

The isothermal planes that are shown in Figure 3.5 with different colors can be considered quite flat which means the heat transfer that is vertical to these planes is only in one direction and can be estimated as one dimensional.

It should be noted that heat transfer analysis and U-factor calculation during optimization process could be done using FEM analysis of the same 3-D structural model. However, since it increases the computation time of the process and on the other hand, theoretical calculation is quite accurate and fast, it was decided to use one dimensional heat transfer method that is discussed in section 2.2.4.

3.3.2. Methodology

To design the mechanical strength of the panel, the highest load on the panels shall be assumed, which includes the weight of all products and the workers during loading or unloading. For example, if Ford Transit Connect considered as the targeted vehicle, since the maximum load capacity of the vehicle is 400 kg and cargo size is 2 x 1.25 m then a uniformly distributed loading of 150 kg/m² can be applied with the safety factor of 2. Calculating the stress or deflection of the panel under this load based on an analytical formulation is a difficult problem, requiring many simplifications and unreal assumptions. FEM software such as ANSYS is powerful tool that can help to solve this problem and provide reliable results. Because the optimization process needs the structural calculations to be performed repeatedly for variety of design variable values, programing the FEM software for the desired problem has to be done in a parametric way. Therefore, an ANSYS script file was written for modeling the panel under the given design parameters.

The code reads the initial values from a .txt file as an input, creates the necessary points, lines and areas to build the model, meshes the model with Shell element and applies the desired boundary conditions, such as supports on the bottom of the panel and vertical distributed load on the top surface of the FEM model. The loading is perpendicular to the face of the panel and it is assumed that the panel is mounted on the ground (floor of the truck) so the vertical displacements of all the nodes at the bottom edge of the webs are zero as shown in Figure 3.6. Also, due to symmetry and to avoid free body displacement of the panel only the center node of the panel is fixed in the horizontal directions. After solving the problem, the maximum equivalent stress (Von Mises) of the panel under the applied load has to be found and written in another .txt file as the result of analysis. The output result from ANSYS is the constraint value for the

optimizer based on the given initial parameters, which should be less than the allowable flexural stress of the material.

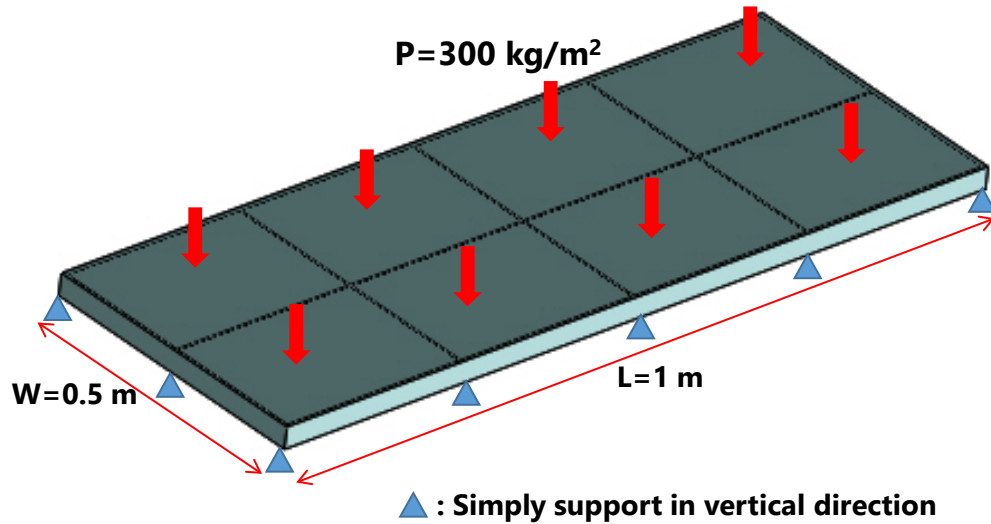


Figure 3.6. Schematic of applied load and boundary condition to the panel

Material properties for the body of panel and insulating material that are used in this project are provided in Table 3-5.

Table 3-5 Properties of the materials being used in insulation panel design [57,38]

	Material	Young modulus	Poisson Ratio	Thermal Conductivity	Allowable flexural stress	Density
Panel body	PVC plastic	2 GPa	0.4	0.15 W/mK	2.5 MPa	1400 kg/m ³
Insulation	Aerogel Blanket	-	-	0.015 W/mK	-	130 kg/m ³

On one hand, the modular geometry of the structure provides mechanical support for the panel; on the other hand, the high thermal conductivity of the material used in the structure acts as a thermal bridge and reduces the thermal resistance of the insulation panel, which in turn leads to higher energy loss during operation. In

conclusion, there is a trade-off between mechanical strength and thermal performance of the insulation panel. This is where optimization of the problem could help to find the best solution.

ANSYS allows the user to perform optimization algorithms to minimize the mechanical stress or deflection in a structure. MATLAB also has a very sophisticated and comprehensive optimization toolbox that can be used in order to optimize different kinds of engineering problems; however, it is not a finite element method software. It is a powerful program that provides different optimization algorithms besides the possibility to define new optimization algorithm. In conclusion, coupling ANSYS and MATLAB can create a powerful tool to solve optimization problems that associated with complicated FEM analysis. Since the user can change the optimization and geometry parameters in the same algorithm, different parameter's effect on the results can be observed. One of the main advantages of coupling ANSYS with MATLAB is that this method is done automatically and user intervention is not required until a stopping criterion is satisfied and the final solution for the problem has been found [59].

Different optimization algorithms are available in the optimization toolbox of MATLAB. Genetic algorithm has been selected to optimize the reinforcing structure of this study because it is a global optimizer and capable of doing multidimensional search in a space defined by different design variables and includes so many local minimums. Genetic algorithm efficiency has been proved in variety of scientific fields experimentally [58]

A genetic algorithm uses a group of variables, called individuals, that are changed and mutated during the process. A chromosome that is described by the design variables represents each individual. Initial population of individuals are selected randomly at the beginning of the process. Based on newly generated variables, the objective function will be evaluated with respect to the constraints, if there are any. Valuable individuals with higher performance will be selected as parents to transfer their genetic materials to the next generation. Probability of selection is higher if the individual shows better evaluation. Selected individuals can be sent to the next generation directly or passed through crossover process. Crossover uses two random parents and

exchange their chromosomes to generate new individuals. Mutation process which introduces new different individuals from the first generation is the next step after crossover that all the individuals have to pass before going to next generation. Population size remains the same during all these processes and generation of the new populations. Repetition of the evaluation process will be stopped if the population converges to a certain level (difference between individuals is smaller than the defined tolerance) or maximum number of generation is reached [58].

It is noteworthy that a genetic algorithm is not deterministic and in different runs, one might get slightly different results. Thus, no general conclusion can be gained, but some guidelines have been proposed to determine the best type of operator and genetic algorithm parameters and the size of the population, which are mostly based on experiments and trial and error. If a convergence criterion is defined in the algorithm, it will allow the genetic algorithm to stop the search for the global optimum without actually obtaining the exact value of that. In order to reach an acceptable solution, different kinds of criteria can be defined. It can be based on the best individual, the average of the population, the specified maximum number of generations or maximum allowable time for the process [58].

Compared to other optimization methods, a genetic algorithm has many advantages. The most significant advantage of a genetic algorithm is that it can optimize large number of continuous and discrete variables and can deal with analytical functions as well as experimental or numerical data. In spite of that, a genetic algorithm could be time consuming regarding the performance evaluation of each individual. For the case of this study, where the finite element method is used to evaluate the constraint of structural performance, this could be an issue. In fact, if the settings of the genetic algorithm are not properly defined, the run time could exceed a few days. Furthermore, genetic algorithms do not guarantee to find the global optimum and there is no exact way to determine which type of operators and parameter setting would result in the best optimized value. Only through a set of experiments with different parameters, one can observe the effect of various operators and setting on the optimized value and some improvement on the initial configuration can be achieved [58]. Table 3-6 indicates the

genetic algorithm settings used to solve the problem. Further discussion about the effect of each setting on the final results is found in section 3.3.4.

Table 3-6 Genetic Algorithm setting parameters for MATLAB

Parameter	Number of Variables	Population size	TolFun	TolCon	Generations	Mutation rate
Value	6	100	1E-3	1E-3	20	0.05

3.3.3. Coupling ANSYS with Genetic Algorithm

In order to be able to automate the proposed optimization methodology it is necessary to couple optimization algorithm from MATLAB to FEM problem in ANSYS. Similar process has been performed to optimize the weight of a bus structure that is described completely in [59] and used as a reference in this study.

Any FEM problem can be created and solved in ANSYS either by using commands from menus or by running a code in ANSYS Parametric Design Language (APDL). Creating and solving a model by means of APDL has advantages, for example the model can be defined using variables that can be manipulated to define different models. Generally, the variables that are defined to create a parametric model are panel thickness and height, number of webs in longitudinal and lateral directions and the thickness of the webs, as they influence panel mechanical strength. Other variables such as the panel dimensions are defined as constant parameters based on the geometry of the reefer truck that the panel is supposed to be installed in. During the optimization loop, the values of design variables will be changing until the stopping criteria is satisfied. Separate files with text format can be created with APDL to provide the possibility of transferring data such as results or input variables between ANSYS and MATLAB.

Figure 3.7 demonstrates the optimization loop and the output files that transfer information between different steps. All of the created files are placed in the same folder that is introduced to MATLAB and APDL code.

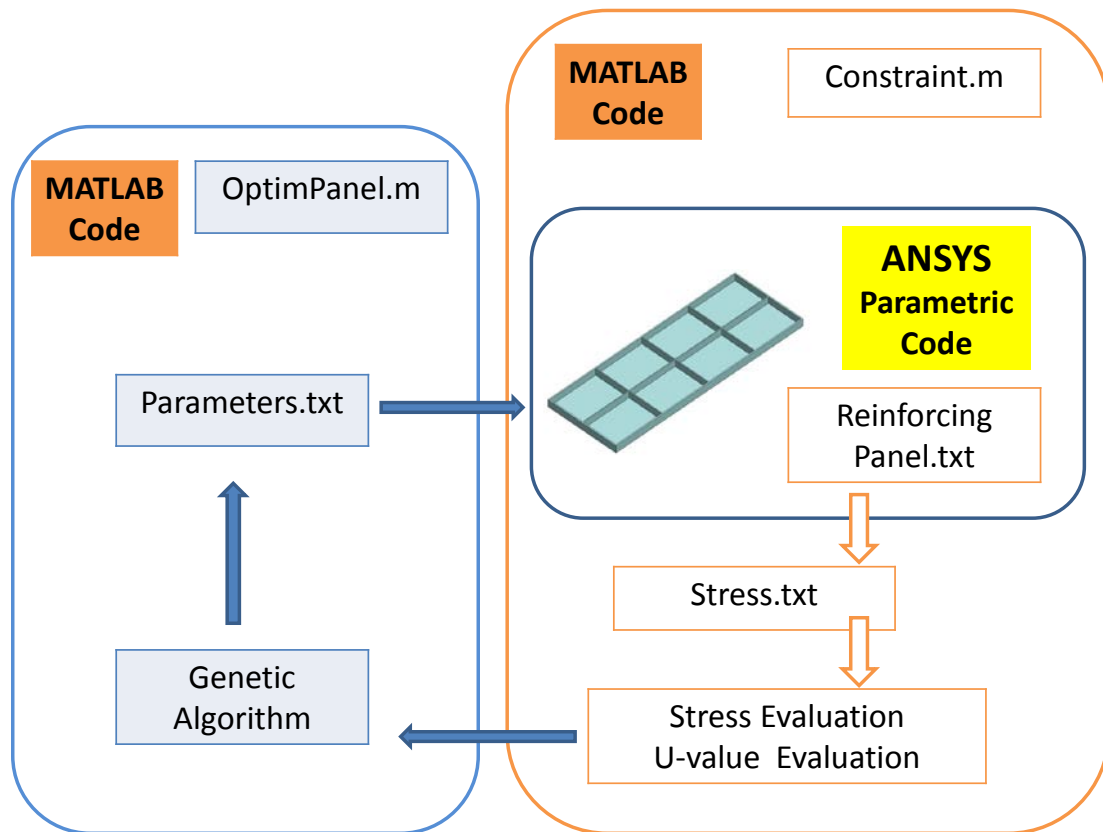


Figure 3.7. Flow chart of the optimization process

Following steps are performed by the optimization algorithm:

The file “OptimPanel.m” that runs the genetic algorithm in MATLAB, needs to evaluate the fitness function and satisfaction of the constraints. Thus, it creates the first set of design variables in the specified bands and recall files “fitnessfunction.m” and “Constraint.m” in a loop for evaluation.

The file “Constraint.m” that supposed to investigate the validity of mechanical and thermal constraints, inserts the values associated to each of the variables in the file “parameters.txt”. After that the finite element model can be run. The finite element model is programmed, by means of APDL, in a text file (“Reinforcing Panel.txt”). This text file gets the values of the variables from file “parameters.txt”. After running the finite element analysis, once the model is solved, the result is stored in a file (“Stress.txt”). This result will be used to evaluate the constraint, which represents the maximum equivalent stress in the panel under the defined load and must be less than the allowable amount for the

material. In addition, U-value of the panel based on the design variables is calculated and compared with reference value by MATLAB code in file “Constraint.m”.

In the next step, the value of all the variables is changed by the genetic algorithm using genetic operators, in order to achieve a minimum in the fitness function. The new values of the design variables are stored and overwritten during each loop in “parameters.txt”. The process will continue until a stopping criterion is satisfied. For more details, please refer to Appendix A. of this report.

3.3.4.Results and Discussion

In order to calculate the stress of the web-core panel under a uniform constant load, a proper mesh should be generated in ANSYS. Mesh generation is one of the most important steps in engineering analysis using a finite element approach. Too many cells may extend the computing time and make the FEM analysis a very long and slow process, while too few cells may lead to unreliable results. The mesh generated in ANSYS for this specific problem is shown in Figure 3.8. In order to find the satisfying mesh of the panel a sensitivity study on the element size is performed for a few different levels of mesh sizes. Less than 2 percent relative difference for equivalent stress at critical points is observed for refining mesh size from 10mm to 5mm while the computation time increases more than 3 times. Therefore, the element sized is selected to be 10mm and using a typical Pentium Dual-Core PC the average computation time for the proposed model is about 5 seconds.

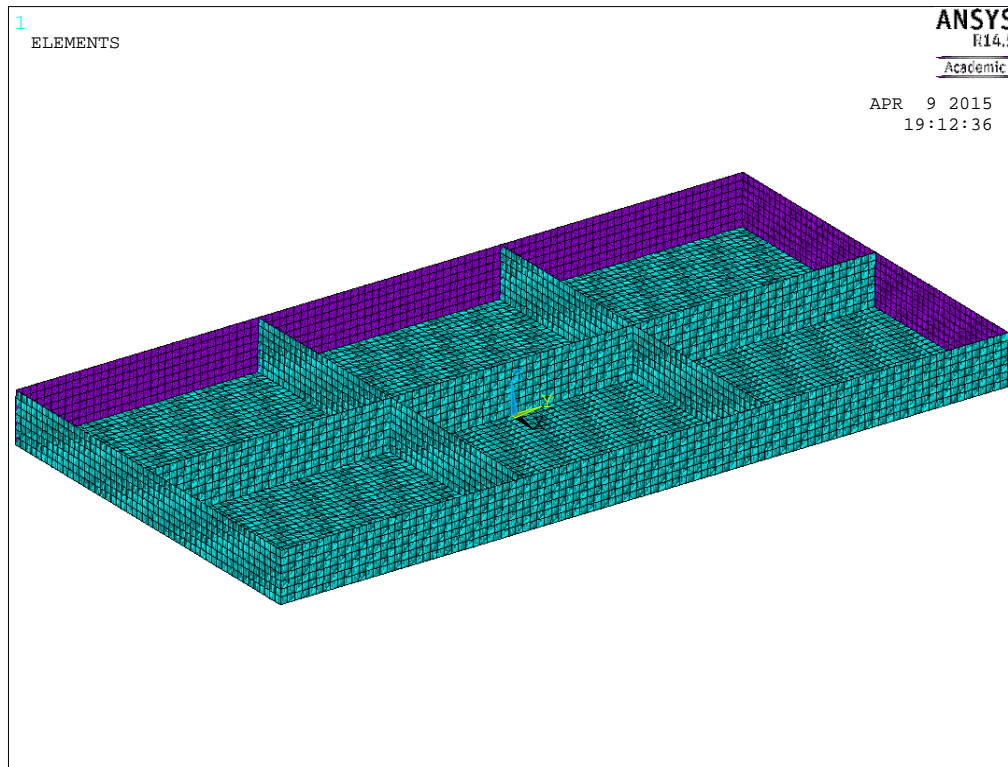


Figure 3.8. Mesh generated in ANSYS [60]

Figure 3.9 shows equivalent stress (Von Mises) in the structure of the reinforcing panel under a uniform load. It is observed that the maximum stress occurs at the junction of webs and the panel surface, which verifies that the webs are supporting the panel against deflection, as there is some stress concentration at this point. In order to reduce the maximum stress, the number of supporting webs could be increased. However, it should be noted that increasing the number of webs could result in higher thermal conductance values since the thermal conductivity of the webs is orders of magnitude higher than that of aerogel blanket.

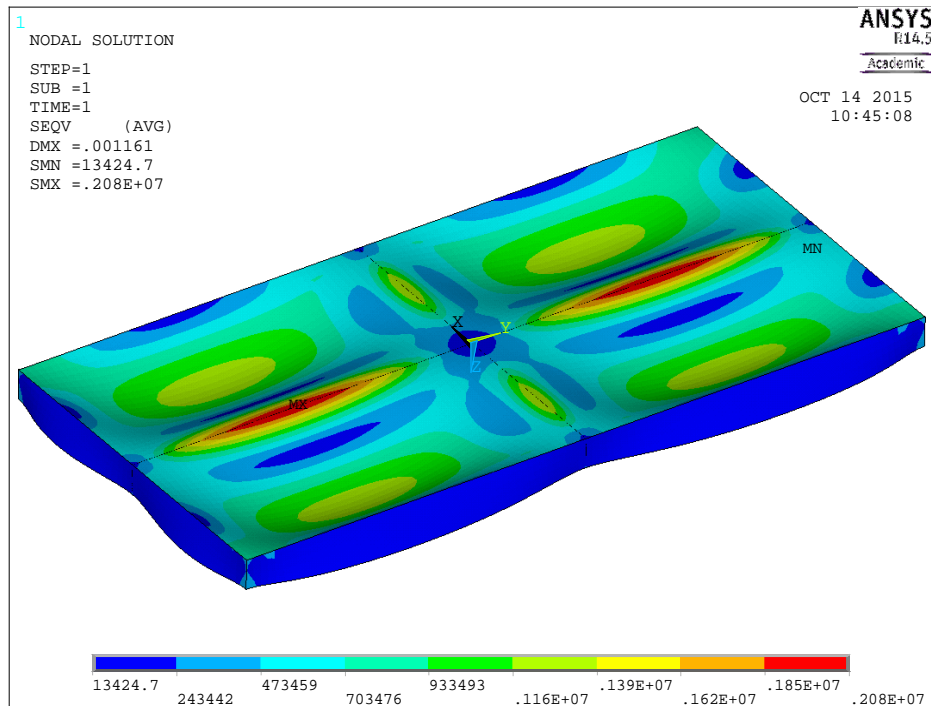


Figure 3.9. Nodal solution by ANSYS, indicating equivalent stress (Von Mises) of the panel

One of the important parameter in the genetic algorithm is population size, which is used to increase the accuracy of the obtained result. Therefore, the value of this parameter is increased by an order of magnitude in a few steps to find the proper size. More accurate results are achieved by increasing the population size, with a higher number of function evaluations and more computation time. Since, for each function count, the GA has to run the ANSYS script one time, which takes about 5 seconds, large population size ended up taking around one full day to run. However, in the end, the value of 100 demonstrated the decent result for this study since brief exploration of the individuals in population showed good coverage of ranges; and thus, was chosen as the initial setting.

The crossover rate is also changed and a crossover rate of 0.8 evolved as the best value for this problem. Decreasing the rate will result in more stagnant generation characteristics. This means that with a lower crossover rate, less change will happen in the genetic characteristics of two consecutive generations. Thus, slower march towards the global optimum value will be observed.

Mutation options specify how the genetic algorithm makes small random changes to the individuals in the population to create mutation children. The initial setting for the mutation rate parameter of the GA in MATLAB optimization toolbox is 1%. Increasing the rate to more than 10% can make the convergence unstable. It is known from the physics of the present optimization problem that there are many local minimums for the fitness function, which can confuse the GA when searching for the absolute optimum of the problem. After a few tries, it was concluded that the mutation rate of 1% is not enough for the GA to jump over the local minimums and consider the diversity of answers. As a result, the mutation value was changed and 5% was discovered to be a good value in order to find better results.

The MATLAB code was run multiple times with the final settings to find the minimum height of the insulated panel and some selected results are shown in Table 3-7. In addition, as an example of obtained results, Figure 3.10 shows the evolution of the height value of the insulated panel. From Figure 3.10 it can be observed that although very big values of the height were obtained at the beginning, once smaller values minimize the fitness function the genetic algorithm converges to a solution.

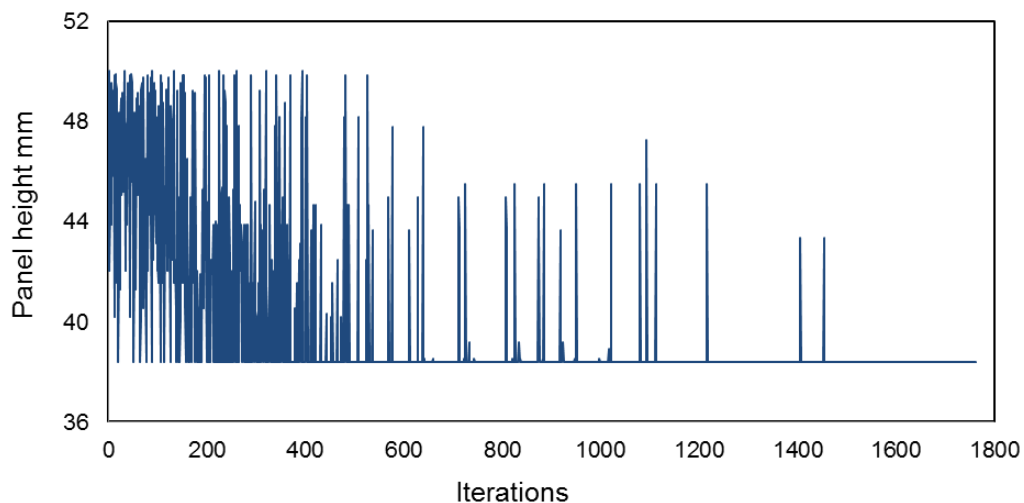


Figure 3.10. Example of the evaluation on the value of the panel height

As mentioned before, one of the shortcomings of the genetic algorithm is that it is not a deterministic method, which means that in different runs the results generated by the genetic algorithm might be different. For this reason, in this study the optimization

process was run multiple times in order to make sure that the results are consistent and GA is not reporting a local minimum as the global one.

Table 3-7 Results of optimization for different runs of MATLAB

Run	h (mm)	t _p (mm)	t _s (mm)	t _r (mm)	n ₁	n ₂	Evaluation Count	U W/m ² K	Weight kg	Webs Heat transfer %	Stress (MPa)
1	46.2	3.3	1.5	1.6	1	3	2300	0.38	3	10	0.982
2	42.4	5.7	1.7	1.7	1	1	3400	0.40	4.4	5	1.602
3	38.4	5	1.6	2.8	3	2	1800	0.50	4.5	18	0.65
4	36.2	5.4	1.6	1.7	2	2	2300	0.47	4.3	9	0.62

The minimum height that is found for the panel as the final answer of optimization process is shown in the last row of the table, which is 36.2 mm. A legitimate reason for being the global minimum is multiple convergences of the algorithm to this value among so many runs. Although genetic algorithm reported some local minimums, as the final answer in other runs, as brought in other rows of the table, the only way to make sure it is not missing the global optimum is running it so many times to increase the possibility of covering all the design space.

As it is observed in Table 3-7, different results for height and thickness of webs, thickness of surrounding structure, thickness of base plate, the number of webs placed along the length (n₁), and the number of webs placed along the width (n₂) are reported that do not indicate the minimum possible height of the panel, but can be interpreted as good solution to the problem. This is due to the fact that local minimums of this problem also have some advantages which can be used by the designer. For example, the first row of the Table 3-7 introduces a panel that is very low in weight in comparison with other, or the panel that is shown in the second row has the minimum number of webs,

which can be an advantage regarding the manufacturing cost of the panel. Considering the results, the designer has different choices for the height, thickness and number of webs in the insulating panel. If the required space for the reefer is very limited, it is better to choose the lowest height although a larger number of webs would be necessary, making the manufacturing process harder and more expensive. On the other hand, a thicker panel provides better insulating capability and perhaps more insulating material and higher cost as well

Taking a closer look at the weight of the panels, it can be concluded that the smaller number and thickness of the webs and panel plate would result in lighter panels and consequently less material that can bring the cost of manufacturing down. Also, the smaller height of the panel does not necessarily result in lighter panel as item number 4 is much heavier than item number 1. On the other hand, it should be noted that the deeper panel (bigger height) requires more insulating material which is quite expensive in the case of aerogel blanket and can affect the final cost of insulating panel.

It is mentioned before that a portion of heat transfer from the insulated panel is through the webs since they can create thermal bridges between sides of the panel by having higher thermal conductivity than the insulating material. Calculated results in the last column of Table 3-7 prove this idea and show that structural webs can play a significant role in the thermal resistance of the panel. For instance, item number 3 that has maximum number of webs relative to the other items, conducting bigger portion of heat through the webs up to 18 percent.

It is observed in Table 3-7 that the thickness of the panel is higher than the thickness of the webs. To justify this result, a deeper understanding of the loading distribution and the way the reinforcing panel would bend under load is necessary. The stress concentration over the panel facing plate due to the bending moment under load causes higher stress on the closest elements to this point, while the inner webs are only under a compressive pressure and not bending as shown in Figure 3.9. Since the uniformly distributed load is symmetrical with respect to the web, it eliminates any sort of bending moment on the webs.

It would be beneficial to have a comparison between the minimum thickness of web-core panel that is achieved in this section for aerogel insulating material and the equivalent thickness of a foam-core sandwich panel that provides same amount of U-value. Regarding the thermal properties of insulating material in Table 2-1, thickness of a panel with Polyisocyanurate (PIR) core should be 48mm to provide the U-value of 0.47 W/m²K while expanded polystyrene (EPS) foam requires 76mm of thickness. Therefore, the PIR panel would be only 12 mm thicker than aerogel panel. It is interesting that although aerogel blanket has super insulating properties but necessary reinforcing webs in the structure of its insulating panel for the application of this study reduce its thermal performance and advantages as well. Needless to mention that aerogel blanket cannot compete in price with other insulating materials in the current market.

Chapter 4. Implementation of Modular Insulating Panels

Initial concepts for designing the insulating panel such as selection of insulating materials, required thickness and mechanical structure of the panel were discussed in the previous chapters. The next step is designing modular panels that can be prefabricated in mass production methods that provide faster and better quality insulating panels. Building a full-scale prototype to validate the capability of the developed design for quick and easy installation inside the target vehicle of this project (Ford Transit Connect) is also necessary.

4.1. Modular Panels and Attachment Methods

One of the important parts in the design of a mechanical system is the installation process, since it can affect the final quality of the product and its working life. Also, installation takes time and labor and so may be costly if is not planned properly. As mentioned before, in the traditional method of insulating reefer vans, insulation material and protective layers are built and installed inside the vehicle one after another. Since, in this project insulating panels are supposed to be prefabricated, the manufacturing and installation process are separated, making it much easier and faster for the installer.

Moreover, the modular system of panels would help not only in the installation, but also later during maintenance or repair, since each part of the insulation can be assembled or disassembled from the others individually. For instance, the whole insulation package can include panels for the floor, ceiling, side walls, front wall, and backdoors. Also, if one of the panels is too big to be manufactured or installed based on this arrangement, it can be sliced to smaller sections, i.e. the floor could be made of two parts. However, having separate components in the system requires an attachment method that can hold each part in the right spot. The common way to mount the panels

inside the vehicles is to use normal fasteners such as bolts, screws, or rivets. However, using the metal fasteners would create thermal bridges between inside and outside of the panels, which is not desirable. Also, this process can be time-consuming and requires certain equipment that may not be available to all installers. Therefore, in this section some engineering solutions are proposed for mounting the modular panels inside the vehicle in an easy and quick way, which also avoids thermal bridges.

A French cleat is a common way to mount the cabinets on the wall (Figure 4.1). In this mechanism there are two wedges, one attached to the wall and the other to the part to be hanged. The weight of the cabinet causes the two edges to come together in such a way that they cannot move. The same concept can be used for the attachment of the panels to the walls of the van.

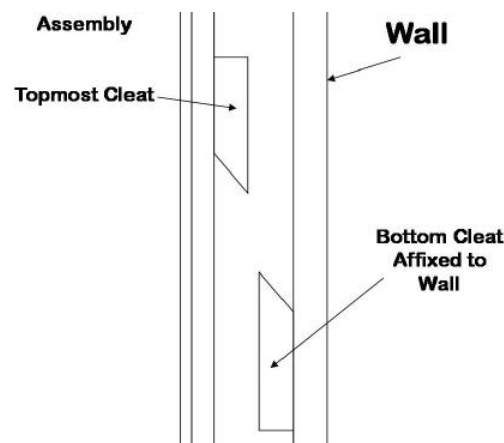


Figure 4.1. Schematic showing the concept of a French cleat [62]

Toggle mechanisms are an often-used clamping method that can pull or push two objects toward or against each other (Figure 4.2). In this mechanism related parts are jointed to each other by hinges that are so arranged that a small force applied at middle point can create a much larger force at the side points. If the angle between the links passes the dead point (zero degree) the mechanism is locked and cannot open up by itself. To deploy this concept for the attachment of panels inside the vehicle, each pair of panels should be jointed together by hinges. For example, if the floor panel is sliced into two parts that are hinged together, they can work like a toggle mechanism to push the side panels back against the walls and tightly hold them in place.

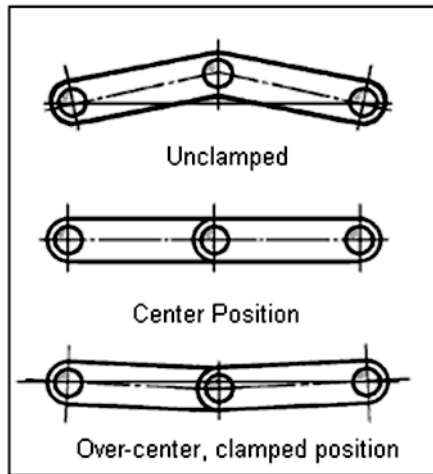


Figure 4.2. Schematic showing the concept of toggle mechanism [63]

4.2. Scanning the Geometry of the Vehicle

In order to design a proper insulating system for the targeted vehicle, the first step was to know the geometry of the refrigerated compartment, its size and space limitations. Unfortunately, a detailed CAD drawing of the Ford Transit Connect is not accessible for research applications. As it is shown in Figure 4.3, the interior design of the vehicle has a complicated geometry, including a lot of curves, angled surfaces, round shapes, holes, beams, and side doors. As such, a simple measurement with ordinary measuring tools is not satisfactory and would not provide enough information to design the insulating panels.



Figure 4.3. Interior view of the Ford Transit Connect, which is to be insulated for reefer applications

Therefore, it was decided to take a three-dimensional image of the vehicle interior body and transform the geometry to a computer model. One of the most accurate and easy ways to do this is to use a portable 3-D scanner. It is possible to bring this device wherever is desired and scan in constrained spaces like the interior or outer surface of objects. A HANDYSCAN 3-D scanner [64] was employed to scan the interior geometry of the van. In order to recognize its position relative to the surface of the object, the scanner requires some positioning targets as small reflecting dots on the surface of the objects. The reflecting targets are small stickers that have to be mounted on the object prior to the scanning process (Figure 4.4). The scanner sees the same

patterns of positioning targets and by triangulation, the scanner is able to determine its position relative to the part (or targets).

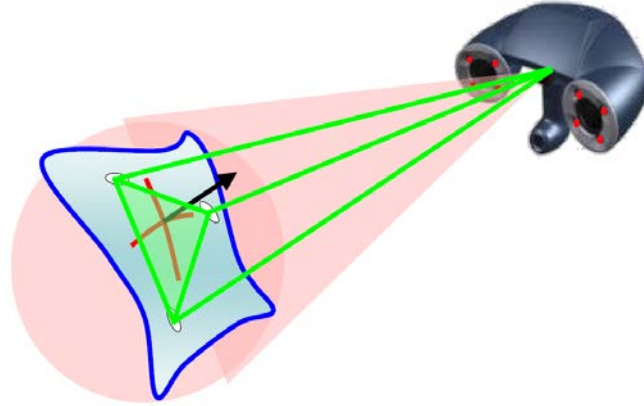


Figure 4.4. Schematic of the 3-D scanner working process[64]

The scanners have automatic surface generation that, during the scanning process, produces the curves in an optimization loop from the collected data. The density and arrangement of the positioning targets can affect the quality of imaging and should be done by an experienced person [64]. The resolution of the camera was set to 2 mm in order to scan the small features of the vehicle body. The presence of small holes inside the body of the van can be confusing for the scanner since there are two or three layers of surfaces at the spot and it is not easy to put the reflector stickers inside the holes. To solve this problem, all the small holes were covered with masking tape. Figure 4.5 shows the scanning process of the Ford Transit Connect.



Figure 4.5. Taking the 3-D image of the vehicle interior surface using a HANDYSCAN scanner

The 3-D scanner is equipped with CAD software (VXelements), which can translate the recorded data to the STL file format, which can be imported by commercial CAD software such as SolidWorks. After some small manipulations to modify the surface errors and remove faulty points of the imported geometry from the 3-D scanner in SolidWorks [65], the surface geometry of the vehicle is available to be used for the insulating panel design (Figure 4.6).

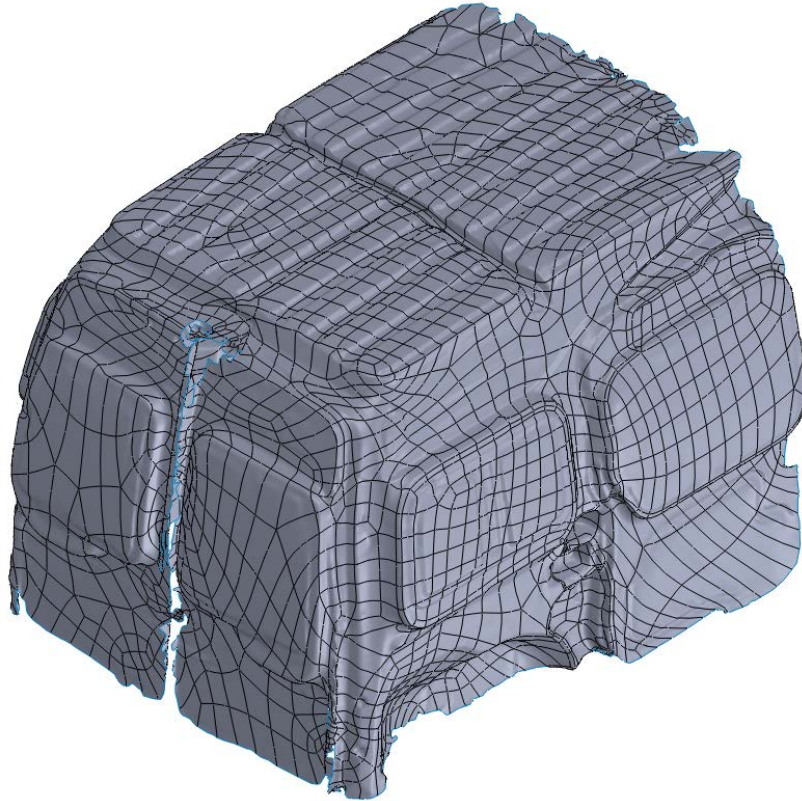


Figure 4.6. Isometric view of the geometry imported to SolidWorks from the 3-D scanner

Since the imported geometry was a skin consisting of many curved patches and other complicated features, it was not easy to directly use it for the modeling of the insulating panels. Also, some errors, such as bumpy and uneven surfaces that are the transformation of flat surfaces, make the model far from reality. Therefore, a secondary model was created based on the original one, but using the geometrical features of SolidWorks such as Extrude, Revolve, Loft, etc. In the new model, which is a solid body, all the surfaces are fitted on the original ones but are quite flat and accurate. Figure 4.7 shows a view of the regenerated model in SolidWorks based on the original imported geometry. During the process of drawing the regenerated model in SolidWorks, some manual measurement was performed on the important sizes of the vehicle body and then the model was modified based on these measurements to make sure the 3-D model and real geometry are in good agreement to each other.

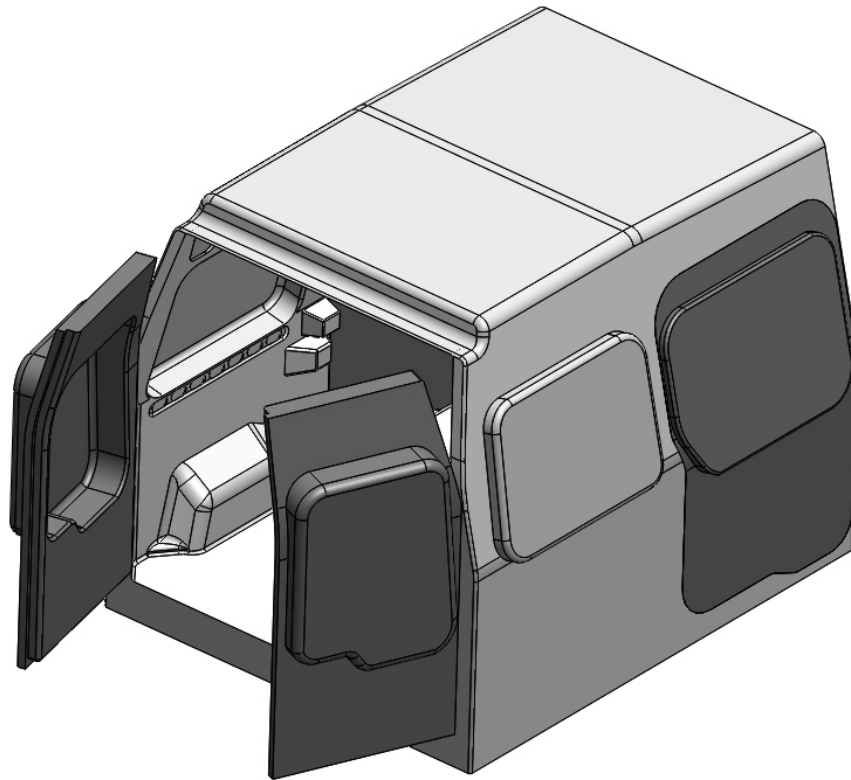


Figure 4.7. View of the regenerated model in SolidWorks based on the original imported geometry from the 3-D scanner

4.3. Scaled Chamber for Experimental Test Setup

In this phase of the project, a small experimental test setup was designed and built to provide some measurements. For example, to prove the proposed CFD model for the air infiltration of the reefer at the time of door opening or to measure the overall heat transfer of the sandwich panels with the selected insulating material, it was required to make an experimental setup similar to the real condition. For more details on the air infiltration testing chamber, please refer to the Appendix B. of this report. Because building the desired chamber in real scale would be very expensive and requires big space and facilities to run the test, it was decided that a scaled-down prototype of the Ford transit loading compartment is built and used for different application.

Design considerations for the test bed panels were different from the real insulating panels for the van. Because there was no exterior structure like the body of

the vehicle to hold the test bed panels, they have to be designed in a way to hold by themselves after assembling. Also, the thickness of panels could not be a scale of real one since it would be very thin and not enough insulation for heat transfer tests. The thickness of insulation was calculated about 50 mm for the real scale and if the prototype is one fifth of the real size, the thickness would be 10mm that is too small to keep the heat load in or outside of the chamber walls. Figure 4.8 shows one of the side panels for the prototype and empty space between the two faces that can be filled with the insulating material. To easily assemble all the pieces, small connecting dowels were used as male parts to mate to female holes.

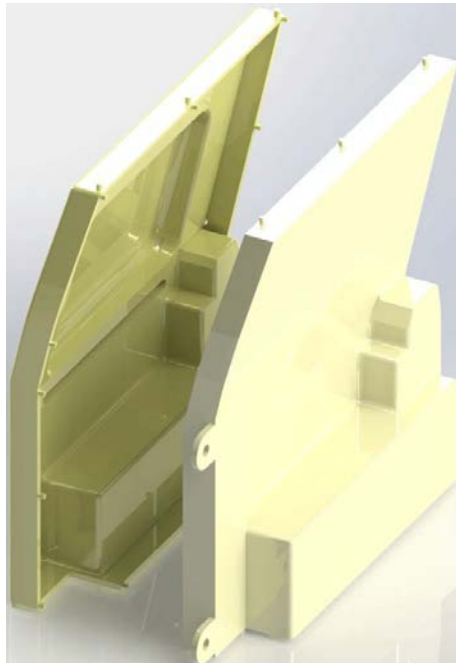


Figure 4.8. Render of a complex panel from the test bed design in SolidWorks

To quickly prototype the test bed, 3D printing was explored. Through exploring different options 3D printer at the School of Mechatronics of SFU were found to be less costly than outside sources, but the limited size of printing forced the scale of the prototype to be very small or each panel had to be made in a few parts and attached to each other later. Other option for the 3-D printing was partnership with Sheridan College in Ontario. Sheridan's largest 3D printer is able to print 3'x2'x3'; having a larger printing area made it possible to print items without the need to separate them into multiple

parts. Sheridan College also used ABS-M30 plastic instead of regular ABS which is more durable. Figure 4.9 shows the complete model of the 3D printed parts.



Figure 4.9. Complete model of the printed prototype after assembling

4.4. Modular Panel Modeling

The next step was to design the insulating panels based on the SolidWorks model. As shown in Section 3.2.3, the thickness of the insulation should be around 50mm or 2 inches. Therefore, for each side of the chamber a panel was designed that covers the whole surface and does not interfere with features on the main body. In order to use the space inside the chamber in the best way and not to waste any volume, the designed panels would have a similar shape to the walls. In this way, panels for the floor, roof, rear doors, sides and front wall were modeled in SolidWorks (Figure 4.10).

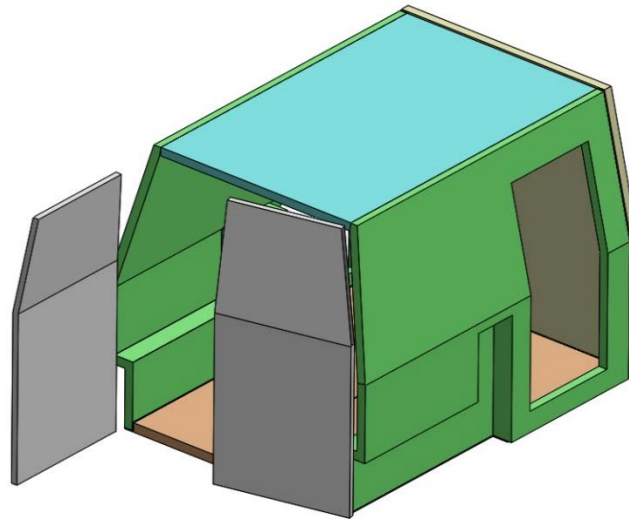


Figure 4.10. SolidWorks model of 2-inches-thick modular insulating panels

Mounting the panels inside the vehicle and securing them is an important part of the design, not only because of its effects on the quality and performance of the insulation, but also due to hard labor and time, which raise the cost of the insulation system. If the design of the panels is done in a way that makes the assembly process easier and faster, it could be a great advance in this industry. Also, it is ideal to have a system in which the quality of the final product is independent of the skills and facilities of the installer. The initial idea to solve these issues was to find a way that the panels can be stand and kept in place by each other. This means that installer does not need to use bolts or other types of fasteners to attach them to the main body of the van and each panel is equipped with a mechanism that makes it able to hold itself and others in the right place. One of the best mechanisms to provide this is the toggle mechanism. It is shown in Figure 4.11 that by having the floor panel in two parts with a hinge in the middle, the installer can press the floor panels down to the ground and at the same time push and hold the side panels against the main body.

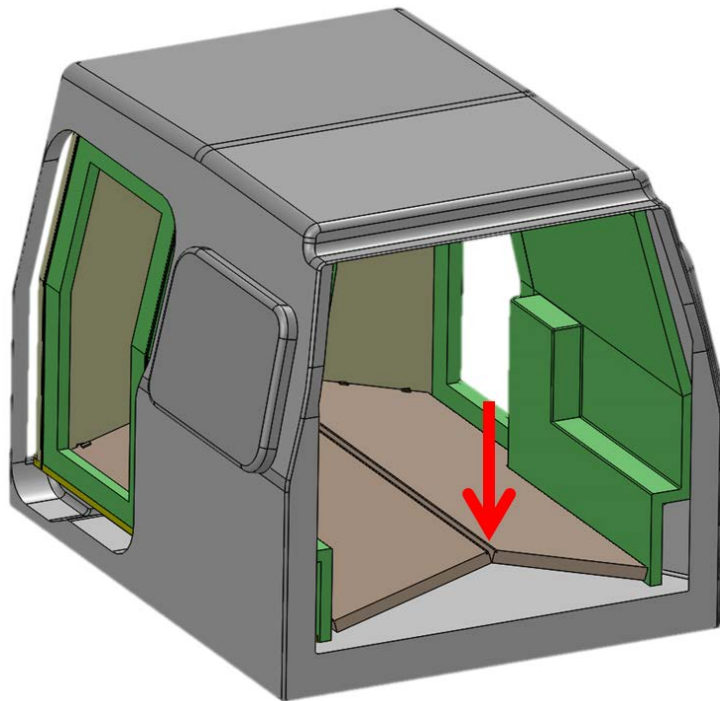


Figure 4.11. Shows toggle mechanism application for holding the side panels with floor panel.

A toggle mechanism is self-locking and once it moves to its dead point, when the floor panels touch the floor, none of the parts can move unless an external force pushes the floor panels up. To avoid this, a small bracket is bolted to end face of floor panels to keep them aligned and in contact with the main body. Also, in real world usage, the weight of the load that is carried by the reefer will help to keep the floor panels in place.

The same method was used for the ceiling panels to hold the tops of the side panels. Because the weight of ceiling panels pulls them down and tends to open the toggle mechanism's lock, an extra edge was added to the sides of ceiling panels to be mounted on top of the side panels (Figure 4.12). Also, it is known that the evaporator box of the refrigeration system is usually mounted on the ceiling of reefer vans. This box is quite heavy (more than 20 lbs.), and needs to be bolted to the steel body of the vehicle. Thus, the ceiling panels will be sandwiched between the evaporator box and the roof of the vehicle, which helps to hold the ceiling panels strongly in place.

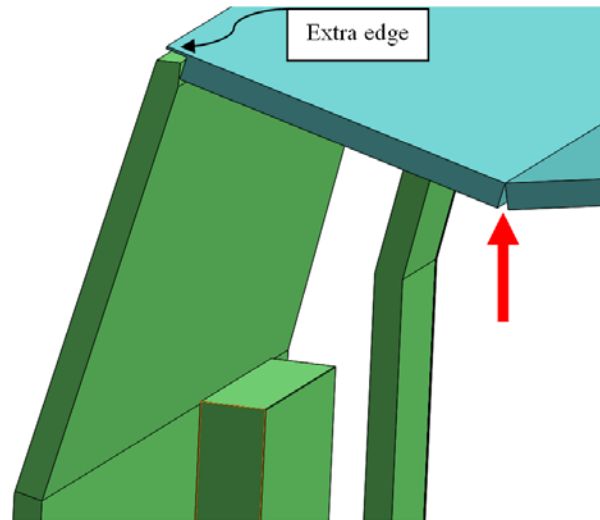


Figure 4.12. Toggle mechanism for the ceiling panels and the extra edge to keep them on top of the side panels.

Apart from holding the side panels by the pressure of floor and ceiling panels, adding some extra joints between the side panels and body of the vehicle would help with the rigidity of the system and make it less likely to be disturbed by vibration when the reefer is driving on the road. Thus, a few small hooks that can attach to holes in the van body are added to the top of the side panels. Consequently, the side panels have to be placed inside the van before assembling the floor and ceiling panels. Figure 4.13 shows the engagement of the small hooks in the holes in the walls. For a better joint between the panels, extra nubs and matched holes can also be made at the side of panels, so that during assembly these nubs and holes are engaged with each other and hold the panels firmly in place.

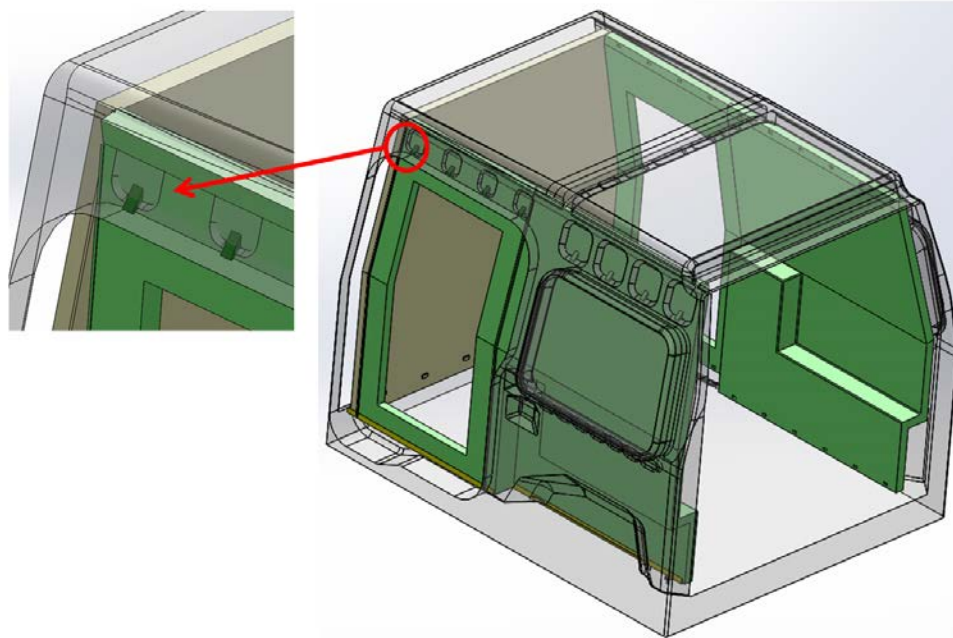


Figure 4.13. Attachment of side panels to the wall by means of small hooks

To hold the front panel in its place and attach it to the others, latch clamps are useful because they are strong and capable of creating large tension forces to draw the edges toward each other. Also, they are very quick and easy to latch, so the installer would be able to fasten them in a few seconds. Figure 4.14 shows the application of these clamps for holding the front panel. These clamps need to be pre-installed on the panels at the time of manufacturing, so the installer only needs to latch them after assembling the panels inside the reefer.

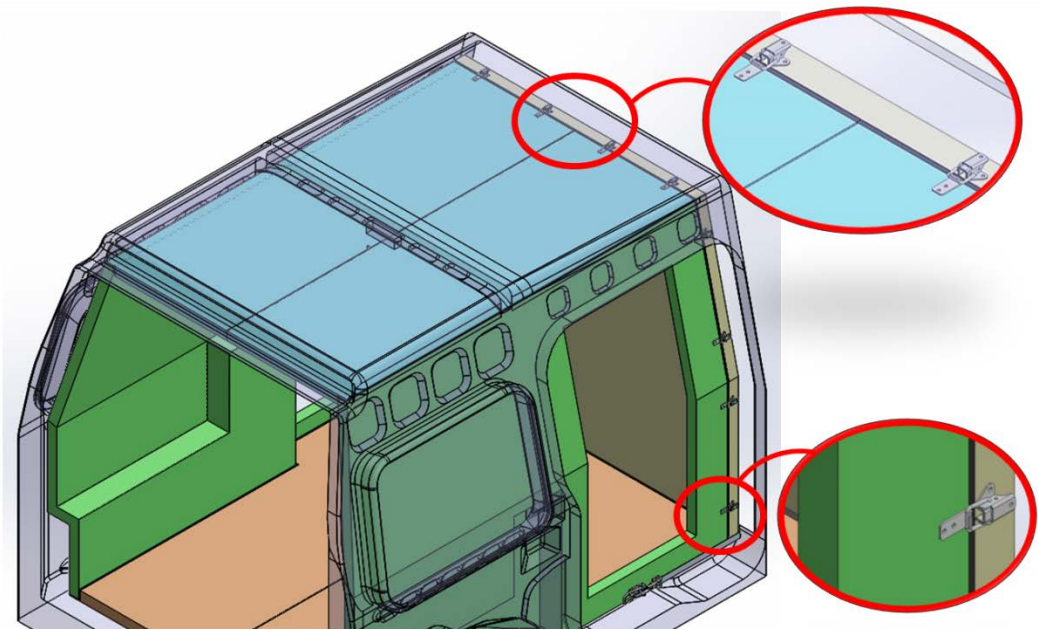


Figure 4.14. Use of toggle clamps to attach and hold the front panels to the side panels.

In summary, the entire assembly process that was discussed in this section is shown in Figure 4.15. Two small insulation panels are designed for the rear doors with the same shape to be mounted on them and will be installed at the beginning or end of the assembly process. A U-shape frame is also shown in the figure, which was created to hold the bottom side of the front panel. This frame is mounted on the floor of the van before assembling the other panels and can be attached to the floor or just clamped to the side panels later. Because of its L-Shape cross section, the frame can support the edge of the front panel and prevent it from getting separated from the floor and side panels. Thus, the front panel is installed after the frame and mounted on top of it. The next step is to bring the side panels inside the van and properly locate them. Floor panels that are attached to each other by hinges along the middle are assembled between the side panels and used as a toggle mechanism to push the side panels against the walls. Finally, the ceiling panels, which are also coupled together with hinges, would be taken inside the vehicle and placed on top of side panels. The ceiling panels also work with a toggle mechanism and push against the side panels. A small bracket will be used to keep the ceiling panels in position, not letting them to bend and fall. Finally, the toggle clamps that are attached to the front panel will be engaged to fix all the panels together. The whole process of assembling the insulating panels should

not take more than one hour, which is much less than the usual time to insulate a reefer van.

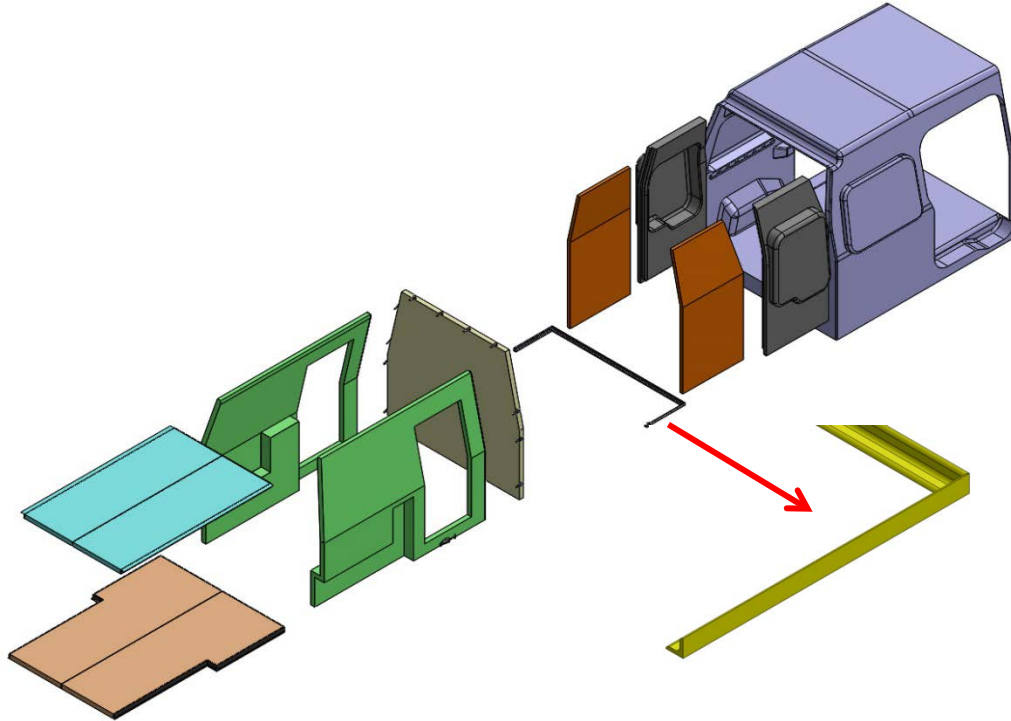


Figure 4.15. Modular insulation panel installation process

4.5. Full Scale Prototype

To examine the feasibility of the different design ideas that have been discussed in this chapter and provide a proof of concept for easy installation of modular insulating panels, it was decided at this stage of project to build a full scale prototype for the targeted vehicle. Considering the available budget and time, there were not many options for the material and production method of the panels. Since manufacturing web-core sandwich panels requires molding of plastic, it is outside of the scope of this project. Also, super insulating materials, such as aerogel blanket, were too expensive at this stage to be used for the complete set of full scale prototype panels. Therefore, foam-core insulation panels were made for the first prototype.

In addition, if the insulating material was applied to the sandwich panels from beginning, the possibility of modifying of them was limited, which is not comfortable for the first prototype. Thus, it was better to make the panels independent of the insulating material and try their size, shape, modularity, and assembling capability first, and then insulate them thermally for use in the real reefer. The best candidate to cope with all these limitations is wood because it is an inexpensive material that is easy to work with and very flexible and able to compensate for possible unexpected issues. Also, wooden panels can be designed to be quite strong and so can tolerate the structural requirements of the system even without filling them with insulating foam. Furthermore, thermal conductivity of the wood is quite low (0.05-0.1 W/(m·K)), which makes it an insulating material; thus later on when the wooden panels are insulated and used as insulating panels inside the reefer van, there will be very little thermal bridging.

To build the wooden full scale panels, it was necessary to redesign the original 3-D model of the modular panels. Considering the 2 inch thickness of the panels, 2"x2" lumber was choose for structural parts and 3/8" thick plywood for the facing of the panels. Figure 4.16 shows a view of modeled wooden side panel in SolidWorks.

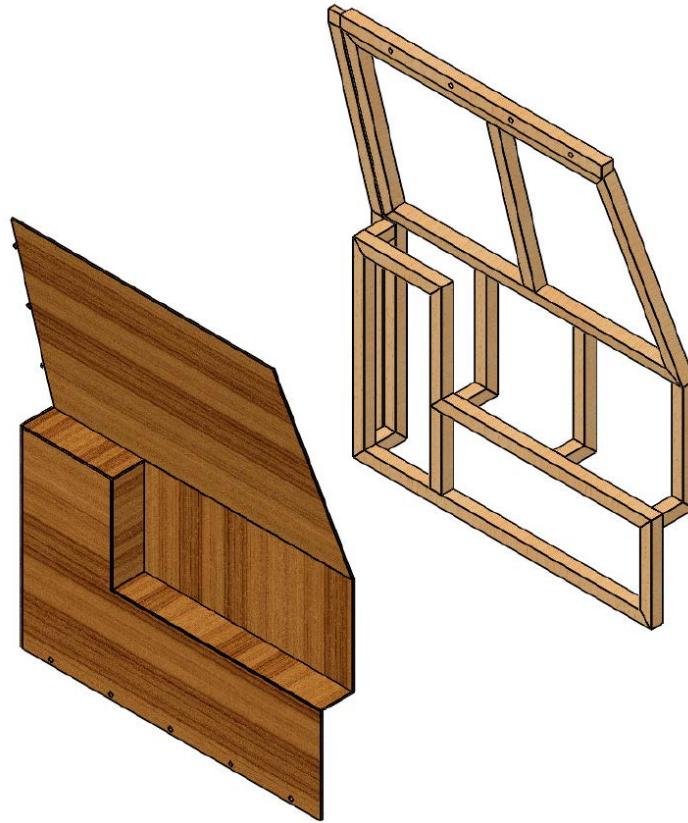


Figure 4.16. View of a modeled wooden side panel in SolidWorks

In the next step, all the necessary material to build the panels was purchased based on the prepared bill of material and in 2 days the manufacturing process was finished. Figure 4.17 shows a picture of a finished wooden side panel.

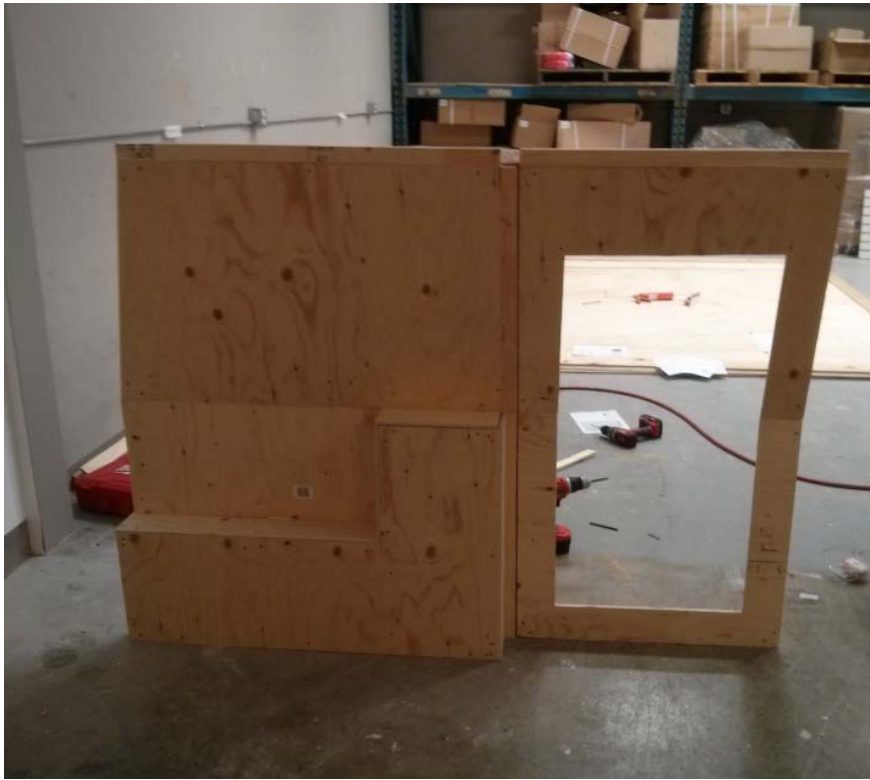


Figure 4.17. Wooden side panel for the Ford transit before installation in the vehicle

Before installation of all the panels together, each panel was located both on its own and beside others inside the vehicle and some small misalignments and mismatches were detected and fixed. Following some shaving and trimming at the edges and corners, all panels were fit inside the van properly and the final assembly of panels was performed in less than 15 minutes with two people, which verified the suitable installation method and low labor time. Figure 4.18 shows the interior view of the Ford transit van with the assembled wooden panels.



Figure 4.18. Final assembly of wooden panels inside the Ford transit van

4.6. Finalizing the Panels and Reefer Installation

To see the performance of the insulation panels in real conditions and investigate possible issues when they are installed in a reefer truck, it was decided to add insulating material to the panels and prepare them for final installation in the Ford Transit reefer. After considering the available insulating materials, the best choices was closed-cell PU foam. Closed-cell PIR is available in the market but comes in rigid boards with certain thickness that did not match with size of the panels. Also, inexpensive glass wool bat and EPS board are common in the industry for reefer insulation, but their insulating

properties are not satisfactory. Aerogel blanket is an excellent thermal insulator, but quite expensive in comparison with PU foams. Closed-cell PU foam is available in spray form and has much better properties than open-cell foam, such as lower thermal conductivity, less degradation, and much higher mechanical strength. Thus, the wooden panels were sent out to a professional insulating company to be filled with closed-cell spray foam [66]. Figure 4.19 shows wooden floor panels after they were insulated with spray foam.



Figure 4.19. Floor panel after being insulated with closed-cell PU foam

It is necessary for the panels inside the reefers to be food grade and washable for reasons of hygiene. FRP (Fiber Reinforced Plastic) and PVC panels are very common facing materials, as well as aluminum and stainless steel sheets for this application. Because metal facing makes insulation panels heavy and not easy for assembling inside small reefer like the Ford Transit, plastic paneling was selected for the facing of panels. Additionally, FRP, which is stronger than other plastics mechanically and chemically, was available at almost same price as others. All the insulating panels

were covered with FRP facing on both sides. To protect the edges on the door opening and the surface of the floor panel from possible damage during loading and unloading of goods, aluminum angles and strips were glued and screwed shallowly on the panels. Figure 4.20 shows the interior view of the van after assembling the insulating panels covered with FRP facing.

Finally, an electric refrigeration system that is designed for mobile refrigeration applications [67] was installed by COOL-IT, the industrial partner for this project. As is shown in Figure 4.20 and Figure 4.21 the evaporator module was attached inside on the ceiling panels and condenser module, which includes the compressor, was installed outside on the roof. This refrigeration system runs on DC 12 volts and has a maximum cooling capacity of 1530 W, which is powered by the battery and alternator of the vehicle.



Figure 4.20. Rear view of assembled insulating panels covered with FRP facing



Figure 4.21. Side view of the insulated van after installation of the electric refrigeration system

Chapter 5. Conclusions and Future Works

A new modular insulating panel design for reefer vans was proposed, designed, and tested. Experimental and analytical studies were performed in order to design and build a full scale prototype of insulating panels for Ford transit connect with the industrial partner of project, Cool-It Hi-Way Services Ltd. As explained in Chapter 1, the traditional methods of applying insulation on the reefer vans suffer from a number of drawbacks including time consumption, high labour cost, low quality, big thermal bridges, and quick aging.

In the new design, insulating panels are prefabricated in the factory, which improves the quality of the product and reduces the installation time from a few days to less than an hour. The labour cost is reduced as well. The concept of composite sandwich panels was used in the new design to increase the strength of the panels besides protecting the core material from negative environmental effects. In addition, modularity of panels makes the installation process much easier in comparison with spraying foam inside the vehicle and enables the user to replace the damaged pieces quickly.

The proposed optimization algorithm in Chapter 3 can be generally used for selecting the insulating material and its thickness for any type of reefer van based on the energy cost and ambient conditions. Furthermore, it was shown that to use super insulating materials such as aerogel blanket, a web-core sandwich structure is necessary to protect the soft core against mechanical loads. The minimum possible thickness of these panel is also calculated considering the thermal bridges of the web structure and the required thermal and mechanical resistance.

To validate the structural performance of present modular design, the interior geometry of the targeted vehicle was 3-D scanned and modeled in SolidWorks, which was used to draft the wooden prototype of insulating panels. The finalized insulated

panels were installed inside the reefer van and its structural performance was examined in road conditions.

Future Works

The following directions can be considered as the continuation of this project:

1. The proposed insulation method in this work can be applied to a variety of commercial vans in different sizes. However, since the geometry, size, and application of them are different; more work is required to find the best design for each case and match the proposed techniques for installation.
2. The presented method to build the insulation panel prototype is suitable for production of initial samples and does not guarantee the high quality and profitability of the product. To achieve better results, mass production methods for manufacturing sandwiched insulated panels has to be considered. This includes thermoforming or molding the exterior layers of the panels from proper plastic materials or cutting the desired geometry from prefabricated sandwich sheets.
3. Although, many research projects have been carried out on the insulating materials for refrigeration application, proper characterization of them under various humidity and temperature conditions is still not well understood. The characterization of thermal resistance decay during temperature and humidity cycling would be another remarkable contribution to this industry.

References

- [1] Tassou, S.A., De-Lille, G., Ge, Y.T., “Food transport refrigeration – Approaches to reduce energy consumption and environmental impacts of road transport,” *Applied Thermal Engineering*, Vol. 29, pp. 1467–1477 (2009).
- [2] Gac, A., “Refrigerated transport: what’s new?,” *International Journal of Refrigeration*, Vol. 25, pp. 501–503 (2002).
- [3] Available at: <http://www.epa.gov/ttn/atw/natamain/gloss1.html>
- [4] Argonne National Laboratory. “Analysis of technology options to reduce the fuel consumption of idling trucks,” U.S. DOE(June 2000).
- [5] According to the International Energy Agency (“IEA”) report available at: <http://www.worldenergyoutlook.org/weo2012/>
- [6] ATP agreement, available at: <http://www.unece.org/trans/main/wp11/atp.html>.
- [7] Chatzidakis, S.K., Chatzidakis, K.S., “Refrigerated Transport and Environment”, *International journal of Energy Research* (2003).
- [8] Macchi-Tejeda, H., Opatova, H., Guilpart, J., “Contribution to the gas chromatographic analysis for both refrigerants composition and cell gas in insulating foams – Part II: Aging of insulating foams”, *International Journal of Refrigeration*, Vol. 30, pp. 338–344 (2007).
- [9] Mukhopadhyaya, P., Bomberg, M.T., Kumaran, M.K., Drouin, M., Lackey, J.C., Van Reenen, D., Normandin, N., “Long-term thermal resistance of polyisocyanurate foam insulation with impermeable facers”, *NRC Publication Archive* (2002).
- [10] Bomberg, M.T., Kumaran, M.K., “Use of Field-Applied Polyurethane Foams in Buildings”, *Construction Technology Update* no. 32 (Dec. 1999).
- [11] Available at <http://kingtecusa.com/wp-content/uploads/2012/08/typical-spray-foam-application.jpg>
- [12] Mukhopadhyaya, P., Kumaran, M.K., “Long-Term Thermal Resistance of Closed-Cell Foam Insulation”, 3rd Global Insulation Conference and Exhibition, Barcelona, 16-17 October 2008
- [13] Murphy, J., “Long Term Aging of Closed-Celled Foam Insulation”, *Foam Supplies, Inc.*, 12th International Conference on Blowing Agents and Foaming Processes, pp. 313-326 (May 2010).
- [14] Berge, A., Johansson, P., “Literature Review of High Performance Thermal Insulation”, Report in Building Physics, CHALMERS UNIVERSITY OF TECHNOLOGY, Gothenburg, Sweden (2012), Open access to public available at : <http://publications.lib.chalmers.se/publication/159807-literature-review-of-high-performance-thermal-insulation>
- [15] Simmler, H., Brunner, S., Heinemann, U., Schwab, H., Kumaran, K., Mukhopadhyaya, P., Quénard, D., Sallée, H., Noller, K., Küçükpinar- Niarchos, E., Stramm, C., Tenpierik, M.J., Cauberg, J.J.M., Erb, M. “Vacuum Insulation Panels. Study on VIP-components and Panels for Service Life Prediction of VIP in Building Applications”, (Subtask A): IEA/ECBCS Annex 39 High Performance Thermal Insulation (2005), available at: https://www.energie-cluster.ch/admin/data/files/file/file/1042/annex39_report_subtask-a.pdf?lm=1452871097
- [16] “Mechanical Insulation Design Guide - Materials and Systems”, by the National Mechanical Insulation Committee (NMIC), Last updated: 10-03-2013, available at: https://www.wbdg.org/design/midg_materials.php
- [17] Turner, W.C., Malloy, J.F., “Thermal Insulation Handbook”, R.E. Krieger, (1981).

- [18] "Testing and Application of New Phenomenological Material Model for Foam Materials", Last updated: 11-01-2010, available at: <http://www.posterus.sk/?p=3923>
- [19] Li, C.D., Chen, Z.F., Saeed, M.U., "Characterization of hybrid glass wool suspensions and optimization of microstructure and tensile strength of the associated wet-laid mats by various blendings and numbers of beating revolutions", *Materials and Structures*, Vol.49, Issue 5, pp 1861-1869 (2016).
- [20] Vaitkus, S., Laukaitis, A., Gnipas, I., Keršulis, V., Vejelis, S., "Experimental Analysis of Structure and Deformation Mechanisms of Expanded Polystyrene (EPS) Slabs", ISSN 1392–1320 *Materials Science (MEDZIAGOTYRA)*. Vol. 12, No. 4. (2006), available online at: <http://citeseerx.ist.psu.edu/viewdoc/download?doi=10.1.1.543.9083&rep=rep1&type=pdf>
- [21] Jelle, B.P., "Traditional, state-of-the-art and future thermal building insulation materials and solutions – Properties, requirements and possibilities", *Journal of Energy and Buildings* 43 2549–2563 (2011).
- [22] BASF, Neopor Wall Insulation, Ludwigshafen, Germany: BASF SE (2011).
- [23] Dournel, P., Zipfel, L., "Analysis of the Evolution of PIR Foams in the Context of the phaseout of HCFCs", In: *Polyurethanes Expo*, pp. 325–332 (2001).
- [24] Bomberg, M.T., Kumaran, M.K., "Laboratory and roofing exposures of cellular plastic insulation to verify a model of aging", 3rd Symposium on Roofing Research and Standards Development, ASTM STP 1224, ASTM, Philadelphia, pp. 151-167(1994).
- [25] "Ceramic Paint Additive Makes any Paint Insulate", 20-06-2015, available at: http://hytechsales.com/insulating_paint_additives.html
- [26] Rohatgi, P.K., Gupta, N., Schultz, B.F., Luong, D.D., "The Synthesis, Compressive Properties, and Applications of Metal Matrix Syntactic Foams", *JOM* Vol. 63, No.2 pp. 36-42, (January 2011).
- [27] "Home Insulation With the Stroke of a Brush", Last updated: 30-07-2015, available at: http://spinoff.nasa.gov/spinoff2003/er_4.html
- [28] "The Simple and Affordable Way to Improve Efficiency", 20-06-2015 available at: <http://www.insuladd.com/product-info/see-it-work/>
- [29] "Truck Body's Lightweight Panel", 20-06-2015, available at: <http://www.design-composite.com/index.php/en/produkte/truck-bodies>
- [30] SANDWICH PANEL – COMPOCEL VP, 20-06-2015, available at: <http://www.cel.eu/index.php?IDcod=78&lang=tr#prettyPhoto>
- [31] Kistler, S.S., "Coherent expanded aerogels and jellies", *Nature*, 127, p.741(1931a).
- [32] Kistler, S.S., "Coherent expanded Aerogels", *Journal of Physical Chemistry*, 36(1), pp.52-64 (1931b).
- [33] Xu, J., "Is it possible to create a lighter-than-air aerogel?", 07-09-2014, available at: <https://www.quora.com/Is-it-possible-to-create-a-lighter-than-air-aerogel>
- [34] "Aerogel Above the Flame", 01-03-2012, available at: www.aerogel.org
- [35] Rubin, M., Lampert, C.M., "Transparent silica aerogels for window Insulation", *Solar Energy Materials*, 7(4), pp.393–400 (1983).
- [36] Stepanian, C., Gould, G., Begag, R., "Aerogel composite with fibrous batting", Pat. No. US 7,504,346 (2006).
- [37] "Aspen Aerogels Case Studies", 2013, available at: <http://www.aerogel.com/resources/case-studies/>
- [38] Ruben, Bjørn, P.J., Gustavsen, A., "Aerogel insulation for building applications: A state-of-the-art review", *Journal of Energy and Buildings* 43, pp761–769 (2011).
- [39] Wong, C., Hung, M., "Polystyrene Foams as Core Materials Used in Vacuum Insulation Panels", *Journal of Cellular Plastics*, Vol. 44, pp. 239–259 (2008)
- [40] Binz, A., Moosmann, A., Steinke, G., Schonhardt, U., Fregnan, F., Simmler, H., Brunner, S., Ghazi, K., Bundi, R., Heinemann, U., Schwab, H., Cauberg, J. J. M., Tenpierik, M. J., Jóhannesson, G. A., Thorsell, T. I., Erb, M., and Nussbaumer, B., "Vacuum Insulation in the Building Sector. Systems and Applications", (Subtask B): IEA/ECBCS Annex 39 (2005).
- [41] Schwab, H., Stark, C., Wachtel, J., Ebert, Fricke, J., "Thermal Bridges in Vacuum-insulated Building Façades", *Journal of Thermal Envelope & Building Science*, 28(4), 345-355 (2005).

- [42] Russo, A., Zuccarello, B., “Experimental and numerical evaluation of the mechanical behaviour of GFRP sandwich panels”, *Composite Structures* 81 575–586 (2007).
- [43] Vinson, J.R., “The behaviour of sandwich structures of isotropic and composite materials”, Westport: Technomic, CRC Press (1999).
- [44] Torre, L., Kenny, J.M., “Impact testing and simulation of composite sandwich structures for civil transportation”, *Compos Structure*, Vol. 50, pp. 257–267 (2000).
- [45] Kalaprasad, G., Pradeep, P., George, M., Pavithran, C., Sabu, T., “Thermal conductivity and thermal diffusivity analyses of low-density polyethylene composites reinforced with sisal, glass and intimately mixed sisal/glass fibres”, *Compos Sci Technol*, Vol. 60, pp.2967–2977 (2000).
- [46] Chidom, C.C., “Lightweight Sandwich Panels in Cold Stores and Refrigerated Warehouses”, Bachelor’s thesis, HAMK University of Applied Science (2013), open access to public available at: <https://www.theseus.fi/handle/10024/69446?show=full>
- [47] Narayan, P., “Behaviour and Design of Sandwich panels subjected to local buckling and wrinkling effect”, PhD Thesis, Queensland University of technology, pp. 1-5 (2003)
- [48] Available at: <http://hypersizer.com/industry/projects/NASA-Ares-V-Interstage.php>
- [49] Crowley, J., Morse-Fortier, L., Dentz, J., Parent, M., Gibson, L.J., Tonyan, T., Glicksman, L., “Innovative materials and construction systems for energy efficient building envelopes”, *Thermal Performance of the Exterior Envelopes of Buildings Conference*, Vol. 12, pp. 105–113, (1995).
- [50] Casey, R., Briscoe, “Design of Lightweight Web Core Sandwich Panels and Application to Residential Roofs”, PhD thesis, University of Minnesota (2010).
- [51] ASHRAE Handbook-Fundamentals, 2009, available at:
<http://www.ashrae.org/resources--publications/Description-of-the-2009-ASHRAE-Handbook-Fundamentals>
- [52] Sofrata, H., Salmeen, B., “Optimization of insulation thickness using micros”, *Energy Conversion*, Vol. 34, pp.471–479 (1993).
- [53] Arora, J.S., “Introduction to Optimum Design”, 2nd Edition, Elsevier Academic Press, 2004, ISBN: 0-12-064155-0
- [54] Wang, H., Fu, L., Zhou, Y., Li, H., “Modelling of the fuel consumption for passenger cars regarding driving characteristics”, *Transp. Res. Part D: Transp. Environ.* Vol. 13, pp. 479–482 (2008).
- [55] MATLAB and Optimization Toolbox Release 2012a, The MathWorks, Inc., Natick, Massachusetts, United States.
- [56] MATLAB 2012a Help, Optimization Toolbox
- [57] AWWA C900 standard for PVC products available at:
<http://www.awwa.org/store/productdetail.aspx?productId=6899>
- [58] Corriveau, G., Guilbault, R., Tahan, A., “Genetic algorithms and finite element coupling for mechanical optimization”, *Advances in Engineering Software* Vol. 41, pp. 422–426 (2010).
- [59] Gauchía, A., Boada, B.L., Boada, M.J.L., Díaz, V., “Integration of MATLAB and ANSYS for Advanced Analysis of Vehicle Structures”, *MATLAB Applications for the Practical Engineer*, Mr Kelly Bennett (Ed.), ISBN: 978-953-51-1719-3, InTech, DOI: 10.5772/57390 (2014).
- [60] ANSYS® Mechanical APDL, Academic Research, Release 14.5, [Online] available at:
<http://www.ansys.com/Products>.
- [61] Available at: <http://www.builditsolarblog.com/2014/07/small-simple-efficient-ram-promaster.html>
- [62] “French Cleat Screen Hanging Assembly”, 28-08-2009, available at: <http://www.avforum.com/forum/110-diy-screen-section/1163059-attaching-french-cleat-3-4-mdf.html>
- [63] “How toggle Action Work”, 20-06-2015, available at: <http://www.mjvail.com/destaco/intropage3.html>
- [64] CREAFORM 3-D scanner training script, November 2010, available at: www.creaform3d.com

- [65] SolidWorks 2013, x64 Edition. Available
at: <http://www.solidworks.com/sw/education/education-software-mcad.htm>
- [66] Quik Shield 112 2 lb Spray Foam Insulation, August 2013 Spec. available at:
<http://swdurethane.com/wp-content/uploads/SWD-Canada-Foamed-in-Place-Insulation-2013-10-10-Final.pdf>
- [67] Battery powered refrigeration units for cargo van, 15-02-2015, Spec. available at:
http://corunclima.en.alibaba.com/product/60341176661-801648850/Battery_powered_refrigeration_units_for_cargo_van.html

Appendix A.

MATLAB Codes for Optimization

Below the MATLAB and ANSYS codes which were used in this project are provided.

Insulation Thickness Optimization Codes:

Cost Function:

```
function f = cost(t)
Ti=0;%Inside temperature
To=30;%Outside temperature
k=[0.15,0.035,0.04,0.022,0.022,0.028,0.3]; %[pvc sheet; EPS;PP
honeycomb;Closed-cell PIR;Closed-cell PU;Open-cell PU; FRP sheet]
R=t(1)/k(1)+t(2)/k(2)+t(3)/k(3)+t(4)/k(4)+t(5)/k(5)+t(6)/k(6)+t(7)
/k(7)%Total thermal resistance
Q=(To-Ti)/R;
d=[10;10;10;5;5;3;10];%Degradation time(years)
Lt=10;%Life time
Fc=4e-5;%Energy cost $/Kj
c=[1000;160;500;180;200;90;5000];%cost/lm of thickness
Fuelcost=Q/1000*Fc*Lt*100*8*3600
Panelcost=Lt*(t(1)*c(1)/d(1)+
t(2)*c(2)/d(2)+t(3)*c(3)/d(3)+t(4)*c(4)/d(4)+t(5)*c(5)/d(5)+t(6)*c
(6)/d(6)+t(7)*c(7)/d(7))

f=Fuelcost+Panelcost
```

Run:

```
t0=[0.002;0.010;0.010;0.010;0.010;0.010;0.003];%thickness of each
layer (mm)
A=[];
b= [];
[t,fval,exitflag,output]= fmincon(@cost,t0,A,b,[],[],[],[],[],@mycon)
```

Constriction:

```
function [c, ceq] = mycon(t)
c(1) = t(1)+t(2)+t(3)+t(4)+t(5)+t(6)+t(7)-0.055;
c(2) = -t(1)+0.001;
c(3) = -t(7)+0.002;
c(4) = -t(2);
c(5) = -t(3);
c(6) = -t(4);
c(7) = -t(5);
c(8) = -t(6);
ceq = [ ];
```

Web-Core Panel Optimization Codes:

Fitness function:

```
function f = fitnessfunction(p)
f=p(1);
```

Optimpanel:

```
LB = [0.02 0.0015 0.0015 0.0015 1 1]; % Lower bound
UB = [0.055 0.006 0.006 0.006 5 3]; % Upper bound
ObjectiveFunction = @fitnessfunction;
nvars = 6; % Number of variables
options=gaoptimset('PopulationSize',100,'TolFun',1e-3,'TolCon',1e-3,
'Generations',10,'Display','iter','MutationFcn',
{@mutationuniform, 0.05});
[x_ga,fval_ga,exitflag_ga,output_ga]=ga(ObjectiveFunction,nvars,[],
,[],[],[],LB,UB,@constraint,options);
```

Constraint:

```
function [c, ceq] = constraint(p)
c(1) = p(1)+p(2)-0.055;
R1=p(1)/0.015/(1*0.5);
R2=p(1)/(0.15*p(3)*2*(1+0.5));
R3=p(1)/(0.15*p(4)*(p(5)*0.5+p(6)*1));
R4=p(2)/(0.15*1*0.5);
Rtot=R4+1/(1/R1+1/R2+1/R3);
u=1/(Rtot*(1*0.5));
c(2) = u-0.5;
c(3)=0.4-u;
p(5)=round(p(5));
p(6)=round(p(6));
fid=fopen('parameters.txt','w');
fprintf(fid,'%12.8f\r\n',p(1)); %height
fprintf(fid,'%12.8f\r\n',p(2));%Tp
fprintf(fid,'%12.8f\r\n',p(3));%Ts
fprintf(fid,'%12.8f\r\n',p(4));%Tr
fprintf(fid,'%12.8f\r\n',p(5));%Nl
fprintf(fid,'%12.8f\r\n',p(6));%Nw
fclose(fid);
!"C:\Program Files\ANSYS Inc\v145\ansys\bin\winx64\ansys145.exe" -
b -i "C:\Users\alabbani\Desktop\Masoud\Optimization course\Project
2\Ansys files\reinforcingpanel.txt" -o
"C:\Users\alabbani\Desktop\Masoud\Optimization course\Project
2\Ansys files\output.txt"
fid=fopen('stress.txt','r');
s1=fscanf(fid,'%s',inf);
fclose(fid);
s=str2num(s1);
c(4) = s-2.5e6;
```

```
ceq = [ ];
```

ANSYS script, Reinforcingpanel:

```
/PREP7
*SET,l,1
*SET,w,.5
*SET,e,2e9
*SET,nu,.4
*DIM,p,,6,1
*VREAD,p(1),parameters,txt,,ijk,6,1
(lf7.6)
*SET,h,p(1,1)
*SET,tp,p(2,1)
*SET,ts,p(3,1)
*SET,tr,p(4,1)
*SET,nl,p(5,1)
*SET,nw,p(6,1)

ET,1,SHELL181
MPTEMP,,,,,,,,
MPTEMP,1,0
MPDATA,EX,1,,e
MPDATA,PRXY,1,,nu
sect,1,shell,,
secdata, tp,1,0.0,3
sect,2,shell,,
secdata, ts,1,0.0,3
sect,3,shell,,
secdata, tr,1,0.0,3

RECTNG,-w/2,w/2,-1/2,1/2,
K, ,0,0,0,
K, ,0,0,h,
LSTR,5,6
ADRAG,1,2,3,4, , ,5
AGEN,nl+1,2, , , ,1/(nl+1), , ,
AGEN,nw+1,3, , , ,-w/(nw+1), , , ,
APTN,ALL

LESIZE,ALL,0.01, , , ,1, , ,1,
ASEL,S,LOC,Z,0,0
SECNUM,1
AMESH,ALL
ASEL,S,LOC,X,-w/2
ASEL,A,LOC,X,w/2
ASEL,A,LOC,Y,-1/2
ASEL,A,LOC,Y,1/2
SECNUM,2
AMESH,ALL
ASEL,A,LOC,Z,0,0
ASEL,INVE
SECNUM,3
AMESH,ALL
```

```
LSEL,S,LOC,Z,h
DL,ALL,,UZ,
NSEL,S,LOC,Z,0
NSEL,R,LOC,X,-.005,.005
NSEL,R,LOC,Y,-.005,.005
D,ALL,,,,,ALL,,,,,
ASEL,S,LOC,Z,0
SFA,ALL,1,PRES,1500
ALLSEL,ALL
```

```
/SOL
SOLVE
/POST1
!ETABLE,deflection,U,Z
!esort,etab,deflection
!*get,def_max,sort,,max
!*CFOPEN,displacement,txt
!*VWRITE,def_max
!(1F8.6)
```

```
ETABLE,stress,S,EQV
esort,etab,stress
*get,st_max,sort,,max
*CFOPEN,stress,txt
*VWRITE,st_max
(F20.3)
```

Appendix B.

Air Infiltration Study

The focus of this thesis is the insulation of the reefer van to prevent the heating load getting into the van by conduction heat transfer. However, during loading and more important than that unloading the reefer trucks at the time of delivery, a lot of door opening happen which leads to infiltration of air in the refrigerated compartment. This infiltration would bring moisture and warm air inside that works as the extra heat load on the refrigeration system [1]. More than half of the total heat load on the refrigeration unit and the main cause of the frost formation on the evaporators can be considered as air filtration [2].

The aim of this study was to develop a proper model to measure the air infiltration in a reefer van that provides a deeper understanding of the problem as well as being used later for the application of heat load calculation and design of air barriers such as air curtain. The basic theory for natural convection of fluids at different densities through openings was expressed more than 70 years ago [3]. Due to the weakness of present analytical models the CFD model was used to predict the effect of warm spillage from the cold box to the surroundings. To examine the effectiveness of proposed CFD model, an experimental setup was designed based on the scaled down prototype of a Ford Transit Connect reefer to validate the results of the computational model.

Model Development

Although CFD is generally a three dimensional modelling tool, preliminary work had shown that creating a 3D model to encompass a cold store and its surroundings while still having a small enough mesh to accurately predict the air exchange at the opening required a prohibitively large amount of computer resources.

Therefore, a 2D model was created using Fluent, a general purpose CFD code as shown in Figure B.5.1. The domain of the model contained the volume inside the chamber (initially at 64°C) and a much larger volume outside the chamber (initially at 25°C), to provide a source of cool air for exchange. The volume outside the chamber

was two times larger than the volume inside the chamber to give a good compromise between accuracy and numerical speed. All of the boundaries were adiabatic walls. The numerical mesh was at its finest (2 mm) at the entrance of the door. This was in order to accurately resolve the large shear created by the air during the infiltration. The total number of grid nodes for the problem was 23,000.

Infiltration was calculated for 30 seconds door opening durations from the predicted average temperature inside the cold store.

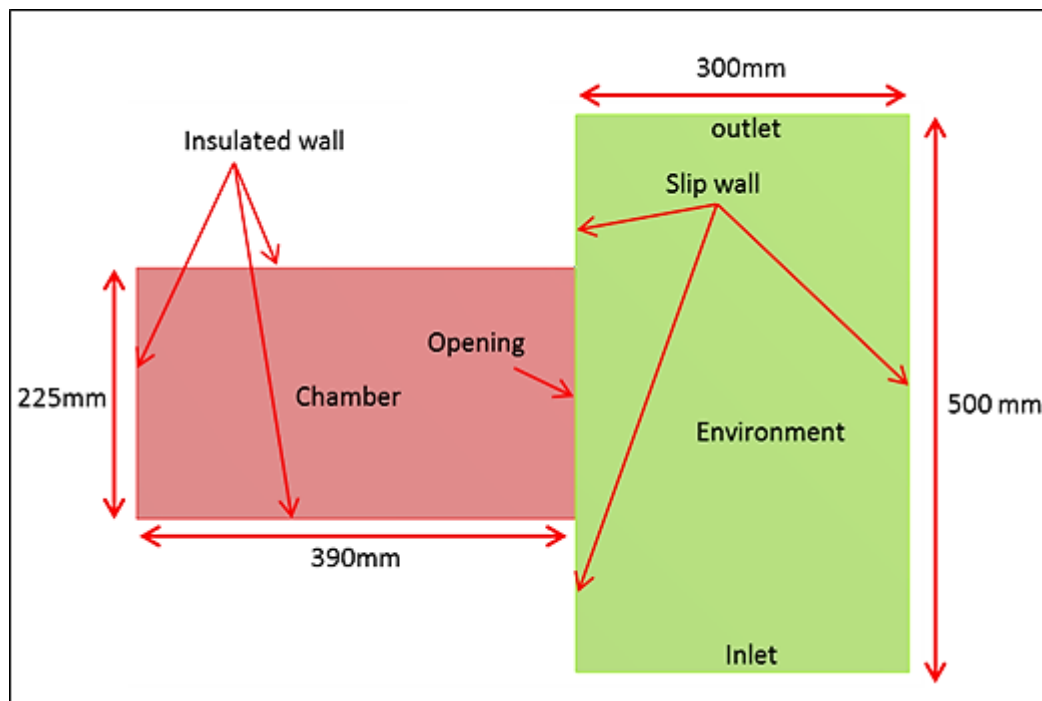


Figure B.5.1. Schematic of a scaled down prototype of a Ford transit connect with overall dimensions

Experimental Setup

Experimental study was carried out on a prototype chamber which is a one-fifth scale model of the Ford Transit with internal dimensions of 0.225m×0.39m×0.23m (Figure .B5.2). This prototype is built by 3-D printing the scaled model of the vehicle image. More details about the modeling and manufacturing of this chamber is discussed in section 4.3. The chamber had an entrance with dimensions 0.23m wide and 0.225m height which was closed off by a push-in door. The thickness of walls (panels) is 25 mm

which is filled with glass wool insulation material. In addition, the chamber was hanged from fishing strings to minimize the heat transfer with environment.



Figure .B5.2. Experimental setup of the infiltrated chamber

A small heater-fan with maximum 500 watt output power with a variable output auto-transformer used to warm the air inside the chamber (Figure .B5.3.). To have uniform temperature distribution before door-opening, two small fans were located besides the heater. At the moment the temperature inside the chamber got to desired point, heater and fans were turn off and the door opened to start the infiltration.

T-type thermocouples were placed inside the chambers in eight locations to measure the temperature distribution and the data was recorded by National Instrument DAQ system using Lab View software.

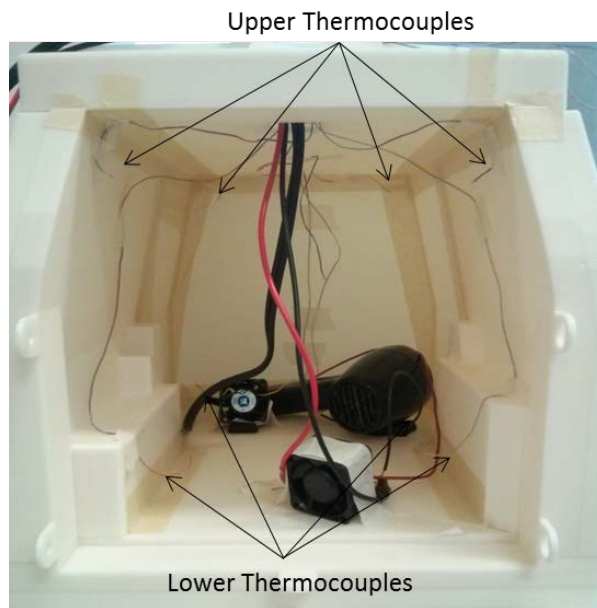


Figure .B5.3. Experimental setup view shows the position of instruments

Results and Discussion

Figure .B5.4 shows the temperature distribution inside and outside of the chamber at 0.6s after opening the door. As is predicted by stack effect or natural convection between the warm chamber and cool environment, the warm air goes out from the top corner and cool air refills the chamber from bottom corner.

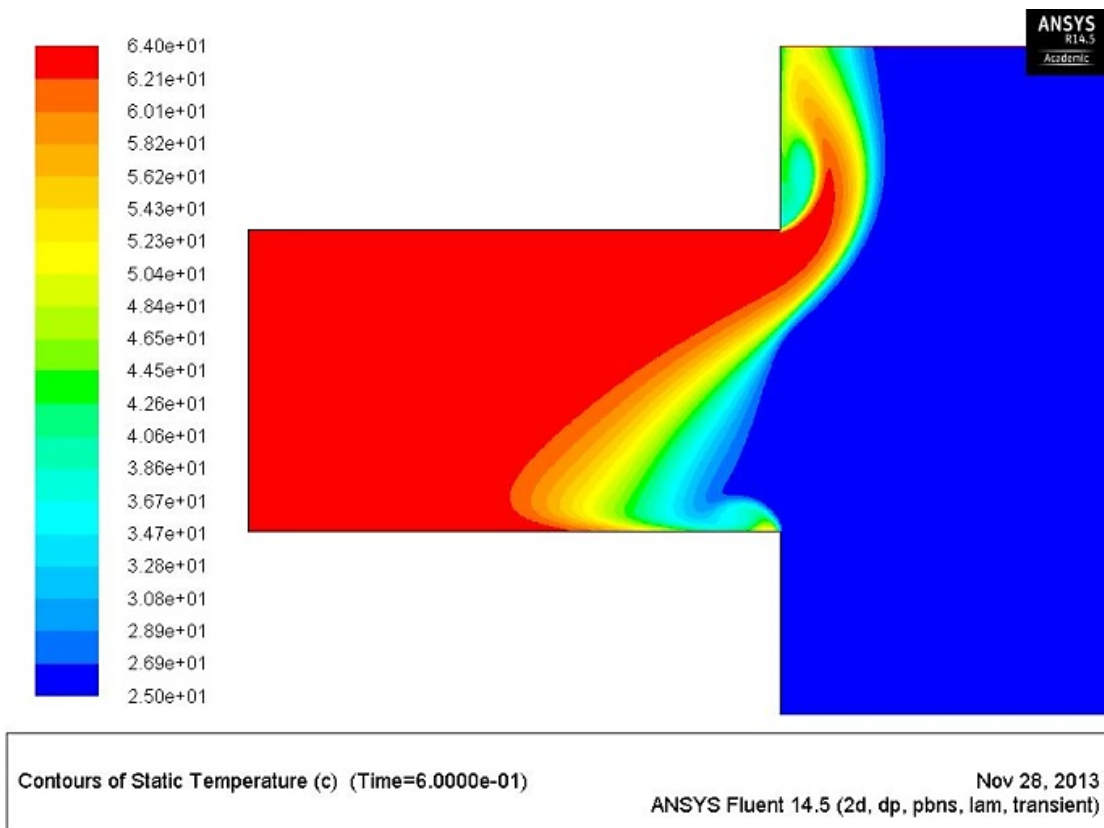


Figure .B5.4. Temperature distribution inside and outside of the chamber 0.6 s after opening the door.

To validate the results of CFD analysis, an experiment was performed in similar condition to measure the temperature change inside the chamber during the first 30 seconds after opening the door. The results for the average temperature inside the chamber, from both the experiment and numerical analysis, are shown in Figure .B5.5.

Although the both curves follow the same trend and the temperature after 30 s is the same, there is a big gap between the results at the beginning of the test. There are two reasons for this difference. The first reason is that, in reality, it takes about 5 seconds to remove the door panels from the chamber and during these few seconds, the heat and mass transfer through the opening is reduced. However, in the CFD model, infiltration of air starts suddenly at the beginning of the analysis and decreases the temperature dramatically and quickly. The second reason could be the thermal inertia of the panels and walls inside the experimental setup, which is not considered in the CFD

model. This inertia releases the heat energy that has been stored in the panels and during infiltration of air slows the temperature reduction inside the chamber.

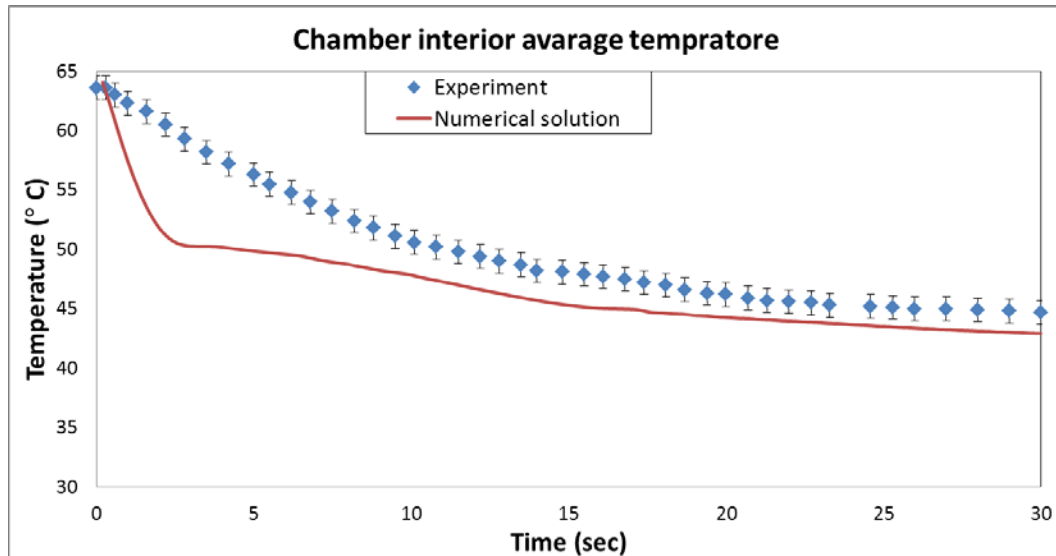


Figure .B5.5. Average temperature inside the chamber for both the experiment and numerical analysis

References

- [1] P. Chen, D.J., Cleland, S.J., Lovatt, M.R., Bassett, “An empirical model for predicting air infiltration into refrigerated stores through doors”, *Int. J. Refrigeration* Vol. 25, pp. 799–812 (2002).
- [2] Boast, M.F.G., “Frost free operation of large and high rise cold storage”, *Proc. Inst. Refrigeration*, Vol. , pp. 1–11 (2003).
- [3] Emswiler, J.E., “The neutral zone in ventilation”, *J. Am. Soc. Htg. Ventil. Eng.* 1 pp. 1–16 (1926).